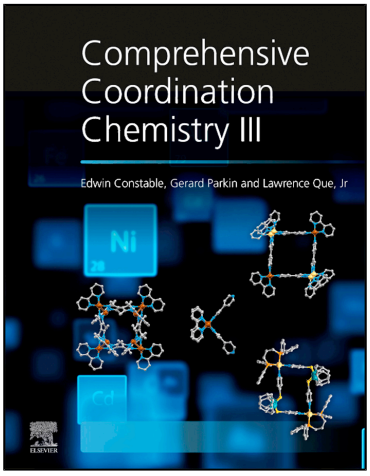

From Webb, D. J.; Hayes, P. G. On the Coordination Chemistry of Bis- and Trisphosphinimine Containing Ligands. In Comprehensive Coordination Chemistry III; Constable, E. C., Parkin, G., Que Jr, L., Eds., Vol. 1, Elsevier, 2021; pp 131–157. https://dx.doi.org/10.1016/B978-0-08-102688-5.00090-8
ISBN: 9780081026885

1.07 On the Coordination Chemistry of Bis- and Trisphosphinimine Containing Ligands

Dylan J. Webb and Paul G. Hayes, Department of Chemistry and Biochemistry, University of Lethbridge, Lethbridge, AL, Canada

1.07.1 Introduction

1.07.1.1 General Introduction

While phosphinimines, or iminophosphoranes, are structurally analogous to imines ($R_2C{=}NR'$; R, R′ = alkyl or aryl), they are much stronger electron donors,[1] and thus, their ylidic character is often depicted by a structure or formula that lacks a formal P=N double bond (i.e. $R_3P^+{-}N^-R'$; R, R′ = alkyl or aryl). Notably, the groups on phosphorous need not be the same, and they often serve as linkers to other donors, thereby creating compounds that can serves as multidentate ligands. In addition, organic linkers are often incorporated into the nitrogen R′ moiety, generating a multitude of possible ancillary ligand architectures. The nature of the connecting group can be distinguished by utilizing the terms *endo* and *exo*, which are intended to indicate if one or more of the phosphorous substituents are (*endo*) or are not (*exo*) part of the linking fragment (**Fig. 1**). This distinction is made in the text by representing *endo* as $R'N{=}P(R)_2$ and *exo* as $N{=}P(R)_3$.

Unlike imines, phosphinimes do not typically participate in π-accepting interactions, instead acting as both σ and π donors through the available lone pair on nitrogen.[1] In the absence of moisture, phosphinimines also tend to be more robust than their imine counterparts, as they are far less susceptible to nucleophilic attack, and are generally stable under strongly reducing conditions.[2] Since phosphorous is an NMR active nucleus ($^{31}P = 100\%$, $I = ½$), ^{31}P NMR spectroscopy has proven to be an extremely valuable tool when characterizing phosphinimine-containing compounds. This is particularly true for phosphinimine-based ligands, as the ^{31}P NMR chemical shift is highly sensitive to its environment, with large predictable changes observed upon coordination to a metal center.

1.07.1.2 Synthesis of Phosphinimines

The Staudinger reaction, named after the German chemist Hermann Staudinger,[3] transforms an organic azide into a phosphinimine ($R_3P{=}NR'$; R, R′ = alkyl or aryl) via reaction with a tertiary phosphine (**Scheme 1**).[4,5] The resultant phosphinimine can be converted into an amine by hydrolysis.

The first step of the Staudinger reaction is generation of a phosphazide ($R_3P{-}N_3{-}R'$; R, R′ = alkyl or aryl) intermediate. Phosphazides are typically transient in nature as they are prone to extrusion of dinitrogen gas, as long as the requisite σ-*cis*oid conformation is accessible.[6] In the absence of water, no further reaction occurs, and given that the process is generally highly selective and the byproduct is a gas, often little to no purification of the phosphinimine is needed.

When an organic azide is not readily available, an alternative procedure, typically referred to as the Kirsanov reaction, can be used to prepare phosphinimines.[7] This route involves the formation of a tertiary bromophosphonium bromide ($[R_3PBr][Br]$; R = alkyl or aryl) by the addition of bromine to a phosphine. An excess of the desired alkyl or aryl amine is then added to the salt in situ (**Scheme 2**). The ammonium bromide is removed via standard filtration techniques. This procedure is often employed if the requisite azide is not accessible, as it can utilize the analogous amine, though it should be noted that complex azides are continuously becoming more available under increasingly safe conditions.[8]

Comprehensive Coordination Chemistry III, 2021, 131–157

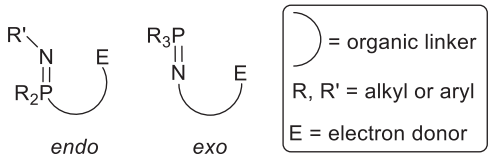

Fig. 1 *Endo* and *exo* phosphinimines.

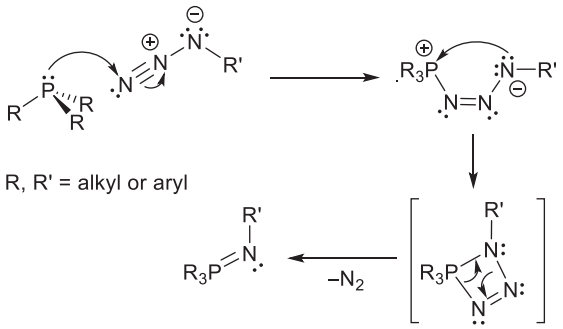

Scheme 1 Synthesis of a phosphinimine via a typical Staudinger reaction.

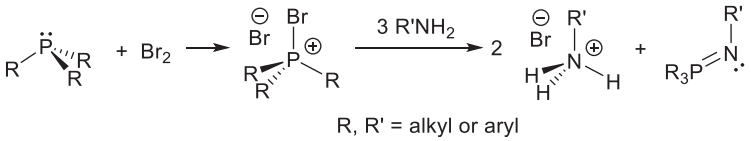

Scheme 2 A typical Kirsanov reaction to generate a phosphinimine.

1.07.1.3 Scope of Review

The modularity, straightforward and inexpensive synthesis, utility of ^{31}P NMR spectroscopy for compound characterization, and electronic properties of phosphinimines has led to the development of a plethora of sophisticated frameworks that have been used to support metals across the periodic table. The rate at which this field has grown, particularly over the past 15 years, renders the time appropriate for a comprehensive review of the coordination chemistry of multidentate phosphinimine ligands. Since the scope of phosphinimines has spread, encompassing many aspects of chemistry, and due to the broad array of ligand frameworks containing a single phosphinimine unit, the following chapter chronicles metal complexes supported by ligands comprised of at least two coordinating phosphinimines that have been reported since 2004. For work prior to 2004, several reviews cover this topic.[2,7,9–11] Monophosphinimine compounds will only be discussed for comparison purposes with their bisphosphinimine counterparts. Due to the large body of research upon, and corresponding review articles that have covered them, the ligand frameworks outlined in Fig. 2 are not included in this contribution; the interested reader is directed to the pertinent literature that does an excellent job addressing this remarkable work.[12–21]

The contribution is organized by ligand type. First, *N,N*-chelating ligands are discussed, followed by pincer ligands, which are subdivided according to donor set: (1) *NCN*, (2) *NNN* and (3) *NON*. Following this, tetradentate ligands, wherein two donors are phosphinimines, are presented. Ligand scaffolds that feature a ferrocene moiety are then addressed, and finally, frameworks that contain three phosphinimines. Within each section, research on a specific family of ligands is discussed together, and where appropriate, separated by type of metal (e.g. transition, rare earth and actinide metals). Ligand classes are represented by "$\mathbf{L_x}$" where x is the number of appearance in this chapter. If there are specific R groups or differing motifs within a set of ligands the distinction may be made by addition of a qualifier next to the number (e.g. $\mathbf{L_{xMe}}$). Unless otherwise stated the ligand abbreviation is intended to represent all variations which occur in the corresponding scheme. When ambiguity exists regarding bonding, the atoms coordinated to the metal are listed at the beginning of the formula. Where there are complicated bonding modes, such as with cyclometalated ligands, an asterisk is used to indicate that it differs from the standard ligand.

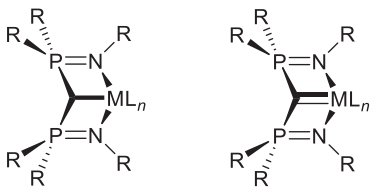

Fig. 2 Methanide and methylidene/carbene types of bisphosphinimine containing ligands that are not included in this chapter.

1.07.2 Bisphosphinimine Ligands

Within this section, all ligands have two phosphinimine donors. These are herein labeled "bisphosphinimine ligands" and are generally based upon two broad classes of previously established systems: pincers and salen ligands. Bidentate *N,N* ligands are also included.

1.07.2.1 *N,N*-Chelating Ligands

In addition to the aforementioned "traditional" ligand types, there are several examples of calixarene and cavitand-based ligands by Dominique, Matt, and co-workers.[22–24] With the bisphosphinimine cavitand-based ligand 5,17-bis(4-methoxyphenyldiphenylphosphinimine)-4(24),6(10),12(16),18(22)-tetramethylenedioxy-2,8,14,20-tetrapentylresorcin[4]arene, $\mathbf{L_1}$, the researchers were able to show that when added to a rhodium containing compound, the resulting complex catalyzed the hydrogenation of olefins with high substrate discrimination by greatly restricting access to the active site.[22] The rhodium catalyst [*N,O*-$\mathbf{L_1}$Rh][BF_4], **1**, was not isolated, but was postulated to be an *N,O*-chelate. Although the same group synthesized several other metal complexes bearing a monophosphinimine ligand,[23] only the calixarene-based scaffolds 25,26,27,28-tetrabenzyloxy-5,17-bis(MesN=PPh_2)calix[4]arene, $\mathbf{L_{2mes}}$, and 25,26,27,28-tetrabenzyloxy-5,17-bis(4-$MeOC_6H_4N{=}PPh_2$)calix[4]arene, $\mathbf{L_{2OMe}}$, were used to produce bisphosphinimine silver and gold complexes (Scheme 3).[24] In the digold complex *N*-$\mathbf{L_{2mes}}(AuCl)_2$, **2**, each phosphinimine was coordinated to a gold chloride, thereby maintaining linear geometry at the two gold centers. The silver species

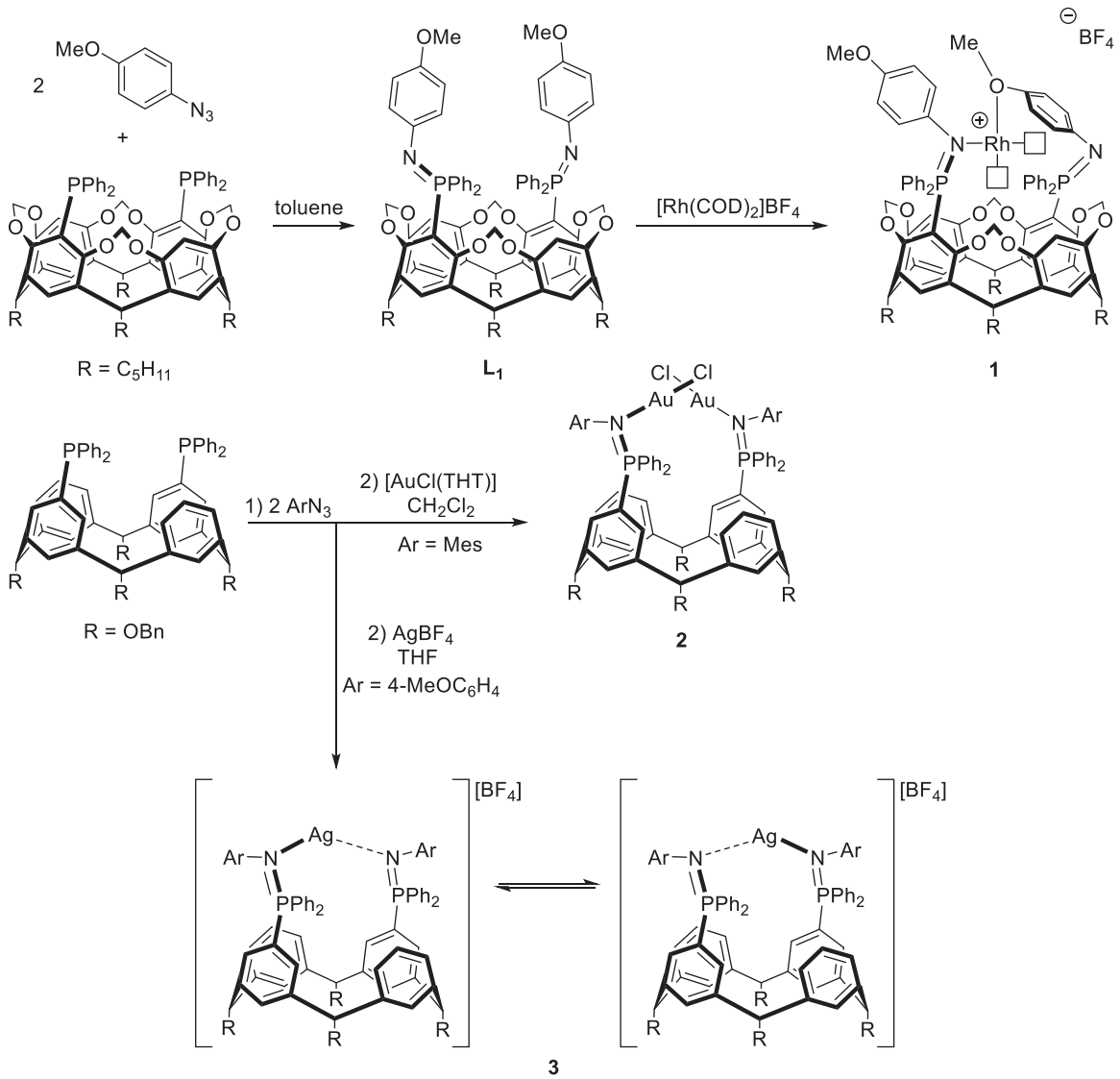

Scheme 3 Synthesis of calixarene rhodium complex **1** with open sites shown, and cavitand-based ligand complexes **2** and **3**.[22–24]

[*N*-$\mathbf{L_{2OMe}}$Ag][BF_4], **3**, also exhibited linearity, but showed fluxional behavior by rotation about the C–P bonds of both phosphinimine groups. The same ligand was combined with palladium(II) acetate in situ and the resulting complex was examined for effectiveness in mediating Suzuki-Miyaura couplings. The palladium species, $\mathbf{L_{2OMe}}Pd(OAc)_2$, effectively catalyzed (0.001 mol% catalyst loading for 1 h at 100 °C, gave 35,100 mol ArPh formed mol(Pd)$^{-1}$h^{-1}) cross-coupling reactions of aryl bromides and chlorides. The authors attributed the good performance of these complexes to the fact that the metal intermediates are extremely sterically crowded, thus facilitating reductive elimination.

Exploring the strongly donating properties of the phosphinimine functionality, Driess et al. synthesized the *N*,*N*-chelating ligand 1,8-(N=P^{n}Bu$_3$)$_2$naphthalene, $\mathbf{L_{3nbu}}$, with *exo* phosphinimine groups to stabilize [ClGe:]$^+$ ([$\mathbf{L_{3nbu}}$GeCl][Cl], **4a**) and [ClGe=S]$^+$ ([$\mathbf{L_{3nbu}}$Ge(Cl)=S][Cl], **5a**) cores; both species contained a chloride counterion (Scheme 4).[25] Similar reactivity was demonstrated with the silicon analogues [$\mathbf{L_{3nbu}}$SiCl][Cl], **4b**, and [$\mathbf{L_{3nbu}}$Si(Cl)=S][Cl], **5b**.[26] Aluminium and gallium complexes were briefly investigated by Sundermeyer and co-workers who focused primarily upon the potential for such ligands to serve as bases and proton sponges. By reaction of 1,8-(N=PMe$_3$)$_2$-naphthalene, $\mathbf{L_{3Me}}$, with two equivalents of $AlMe_3$ and $GaMe_3$, the aluminium and gallium complexes [$\mathbf{L_{3Me}}AlMe_2$][$AlMe_4$], **6a**, and [$\mathbf{L_{3Me}}GaMe_2$][$GaMe_4$], **6b**, were obtained.[27]

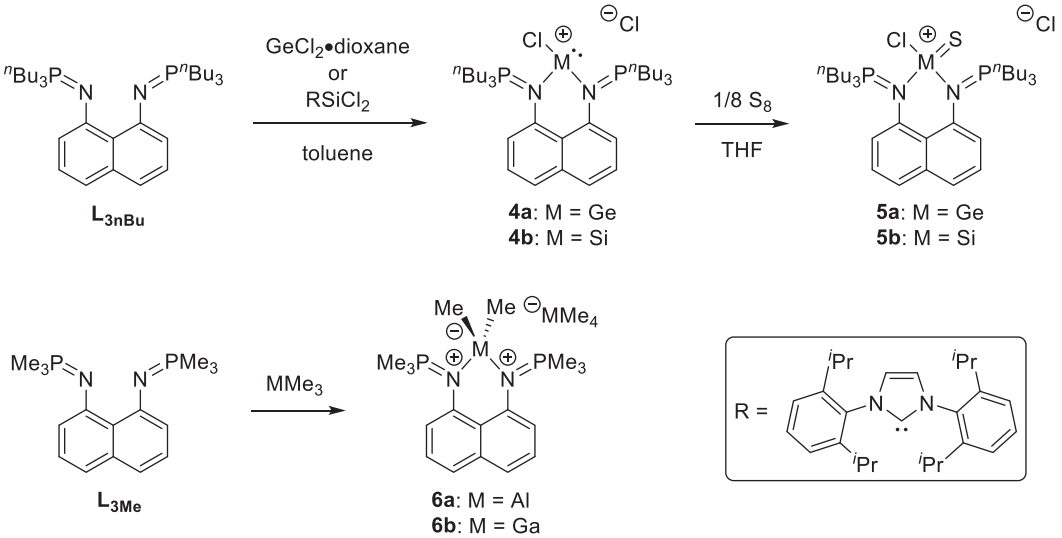

Scheme 4 Main group complexes **4** and **5** prepared by Driess[25,26] and related complexes **6** reported by Sundermeyer.[27]

Using two *exo* phosphinimines and the aromatic scaffold 1,2-(N=PAr$_3$)$_2$benzene, $\mathbf{L_4}$ (Ar = Ph, C_6H_{11}, C_5H_9), Noels et al. produced several copper and palladium compounds (Scheme 5).[28] These complexes were used as catalysts for styrene and cyclooctene cyclopropanation. With styrene cyclopropanation yield was independent of both the oxidation state of copper and the steric environment provided by the substituents bound to phosphorus, though these factors did have an impact upon diastereoselectivity. The less sterically encumbered Cu(I) complexes $\mathbf{L_4}Cu(OTf)_2$, **7b**, gave wider variations of *cis*:*trans* ratios, favoring the formation of *cis* cyclopropane. In the cyclopropanation of cyclooctene, the palladium complexes $\mathbf{L_4}PdCl_2$, **7c**, produced more *exo* cyclopropane, whereas copper species generated greater quantities of the *endo* isomer. Overall, it was concluded that copper was slightly more effective than palladium in both cases, and ligand structure had little impact on catalyst performance.

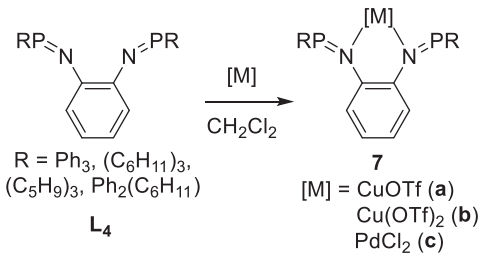

Scheme 5 Synthesis of bisphosphinimine benzene frameworks and copper and palladium complexes thereof.[28]

1.07.2.2 *NCN*-Pincer Ligands

There are a great number of *NCN* pincer ligands that bear two phosphinimine moieties, yet this class is comprised almost exclusively of the aforementioned methanide and methylidene ligands that are not covered within this chapter. As a departure, the *NCN*-pincer ligand, 1,3-(N=PPh$_3$)$_2$xylene, $\mathbf{L_5}$, reported by Stephan, exhibits both anticipated and unusual reactivity with palladium

(Scheme 6).[29] This *exo* ligand, which was prepared via a classic Kirsanov reaction, afforded the palladium species $\mathbf{L_5}$PdCl, **8**, upon introduction to $(PhCN)_2PdCl_2$. Conversely, when the reaction was conducted at 120 °C, and $(COD)PdCl_2$ used as the palladium source, a mixed phosphinimine/aminophosphine bound species, 1,3-$C_6H_3(CH_2N{=}PPh_3)(CH_2NHPPh_2)$PdCl, **9**, was isolated. While the mechanism of formation for complex **9** is unclear, it is worth noting that no conversion from **8** to **9** was observed even after 2 days of heating at 120 °C. When complexes **8** and **9** were treated with a trityl cation a hydride was abstracted from the methylene adjacent to the phosphinimine nitrogen to respectively afford $[1,3\text{-}C_6H_3(CHNPPh_3)(CH_2NHPPh_2)PdCl][B(C_6F_5)_4]$, **10**, and $[1,3\text{-}C_6H_3(CH_2N{=}PPh_3)(CHNPPh_3)PdCl][B(C_6F_5)_4]$, **11**, unusual cationic species wherein the positive charge was ligand-based. Clearly the methylene groups proximal to the phosphinimine are susceptible to hydride extraction.

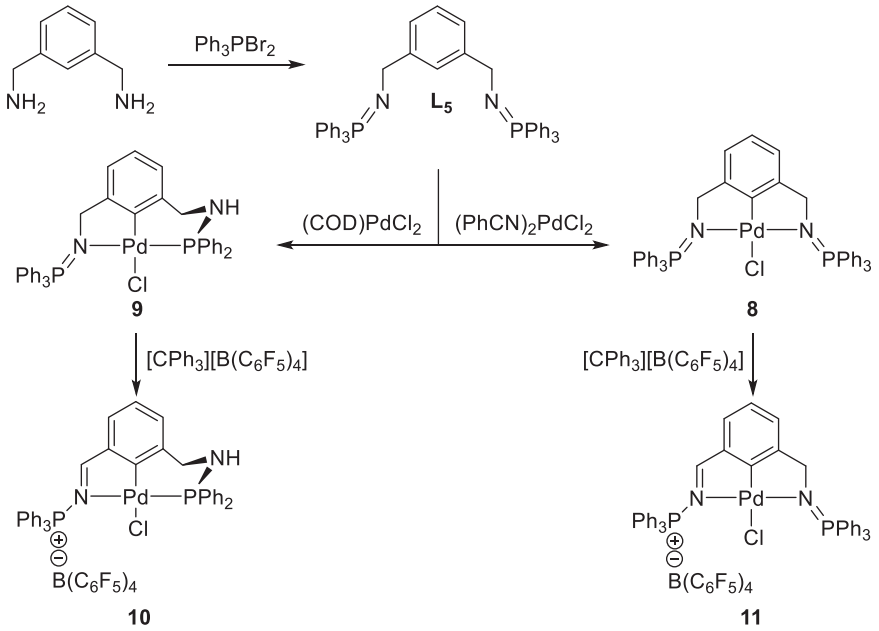

Scheme 6 Non-innocent ligand reactivity in bisphosphinimine pincer complexes of palladium.[29]

More niche analogues of the well-known aliphatic ligands, 1,3-$(S{=}PPh_2)_2$indenylidene, $\mathbf{L_{6s}}$, and 1,3-$(MesN{=}PPh_2)_2$indenylidene, $\mathbf{L_{6n}}$, were synthesized by Bourissou and co-workers.[30] Although they focused predominantly on the phosphine sulphide complex $\mathbf{L_{6s}}Zr(NMe_2)_2$, **12**, they also prepared the zirconium alkylidene $\mathbf{L_{6n}}Zr(NMe_2)_2$, **13** (Scheme 7).

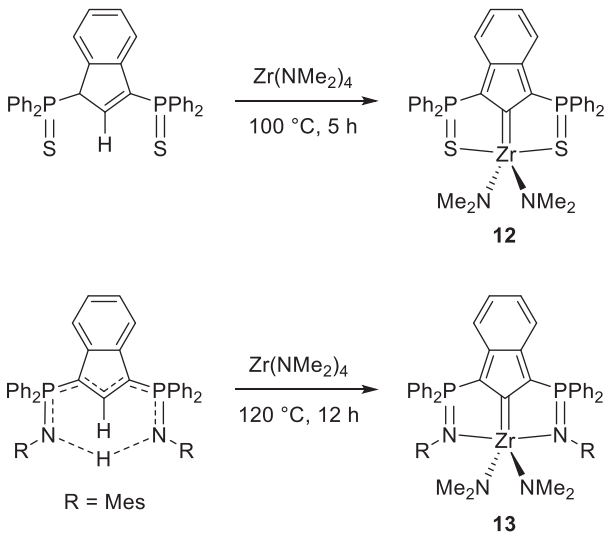

Scheme 7 Synthesis of zirconium indenylidene complexes **12** and **13**.[30]

1.07.2.3 *NNN*-Pincer Ligands

This section discusses *NNN*-pincer ligands and is divided according to the type of metal supported. Several classes of ligand are included; however, each system has a nitrogen-based central donor flanked by two phosphinimines, thereby creating the traditional pincer ligand motif.

1.07.2.3.1 Transition metals

In 2011, Stephan and co-workers reported a family of *exo* bisphosphinimine *NON*- and *NNN*-pincer ligands, O(1,2-$C_6H_4N{=}PPh_3)_2$, $\mathbf{L_{7NON}}$, and RN(1,2-$C_6H_4N{=}PPh_3)_2$ (R = H, $\mathbf{L_{7NH}}$; Me, $\mathbf{L_{7NMe}}$) synthesized via Kirsanov reactions.[31,32] Although a palladium dichloride complex $\mathbf{L_{7NON}}PdCl_2$, **14**, was prepared using $\mathbf{L_{7NON}}$ (Scheme 8), the authors did not investigate the reaction chemistry of this complex given the minimal interaction between the metal center and the oxygen donor.[31] The amide ligands $\mathbf{L_{7NH}}$ and $\mathbf{L_{7NMe}}$ also proved useful in stabilizing a variety of palladium species, though the majority of efforts focused upon the rich chemistry that was revealed when $\mathbf{L_{7NH}}$ was combined with nickel. Specifically, a range of mono- and dinuclear nickel complexes, including $[\mathbf{L_{7H}}Ni(NCMe)_2][BF_4]Cl$, **15**, $\mathbf{L_{7H}}Ni_2Br_3$, **16**, and $\mathbf{L_{7H}}Ni_2Cl_3$, **17**, were isolated (Scheme 8).[31,32] Intriguingly, complex **16** was generated via activation of the C–Br bond of bromobenzene.[32]

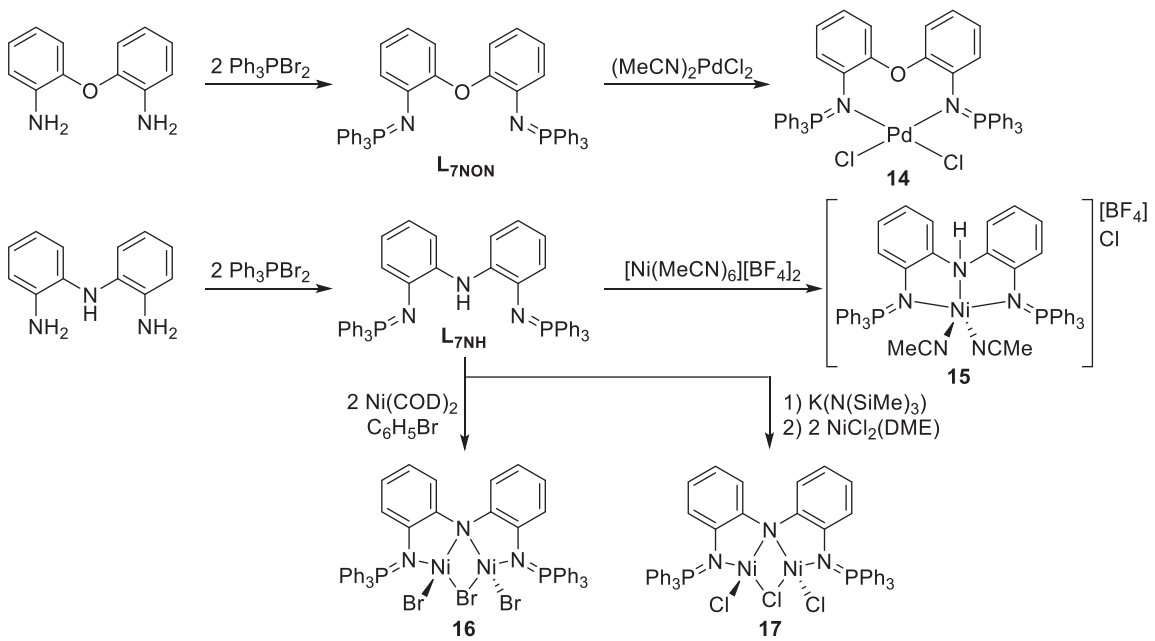

Scheme 8 Synthesis of *NON*- and *NNN*-pincer complexes **14–17**.[31,32]

Additional species that featured the aliphatic backbone R′N($C_2H_4N{=}PR_3)_2$ (R′ = H, $^{H}\mathbf{L_8}$; Me, $^{Me}\mathbf{L_8}$), have also been synthesized.[31,32] Complexes of palladium, $[\mathbf{L_8}PdCl][Cl]$, **18a-c**, and nickel, $[\mathbf{L_{8iPr}}NiCl][Cl]$, **19**, and $\mathbf{L_{8Ph}}NiCl_2$, **20**, were prepared via straightforward addition of the free ligand to the appropriately solvated metal chloride (Scheme 9). Interestingly, variation in the phosphorous substituents dictated whether cationic (**19**, R = ^{i}Pr) or neutral (**20**, R = Ph) species were isolated; subsequent addition of $NaPF_6$ to either **19** or **20** yielded cationic complexes with PF_6 counterions, $[\mathbf{L_8}NiCl][PF_6]$, **21**. Complexes **21** participated in salt metathesis reactions with $LiHBEt_3$ to afford the expected cationic hydride species, $[\mathbf{L_8}NiH][PF_6]$, **22**.[32] When $[\mathbf{L_{8Ph}}NiH][PF_6]$ was heated at 80 °C for 3 h in acetonitrile loss of H_2, along with concomitant cyclometalation of a phosphinimine phenyl group, afforded $[NNNC\text{-}\mathbf{L_{8Ph}}{*}Ni][PF_6]$, **23**. Notably, when R′ = H ($^{H}\mathbf{L_{8Ph}}$) complex **23** was only observed in low yield and was accompanied by nickel black and an unidentified paramagnetic species. However, when R′ = Me ($^{Me}\mathbf{L_{8Ph}}$), the cyclometalated decomposition product was isolated in high yield. Upon exposure of **23** to a second equivalent of $LiHBEt_3$ in bromobenzene $[\mathbf{L_{8Ph}}NiPh][PF_6]$, **24**, the product of C–Br activation, formed. Finally, complex **23** reversibly inserts ethylene into the Ni–H bond to afford, $[\mathbf{L_{8Ph}}NiEt][PF_6]$, **25**.[31,32] The related neutral dinuclear complexes, $\mathbf{L_8}Ni_2Br_3$, **26**, and $\mathbf{L_8}Ni_2Cl_3$, **27**, can be generated under similar conditions to previously reported species bearing an aromatic backbone (Scheme 10).[31,32] Activation of phenyl halides was further investigated using a series of halogenated arenes (C_6H_4EX) which underwent C–X bond activation to produce the cationic complexes, $[\mathbf{L_{8Ph}}Ni\text{–}C_6H_4E][X]$, X = Cl, E = F, **28a**; X = Br, E = H, **28b** (Scheme 10).[31]

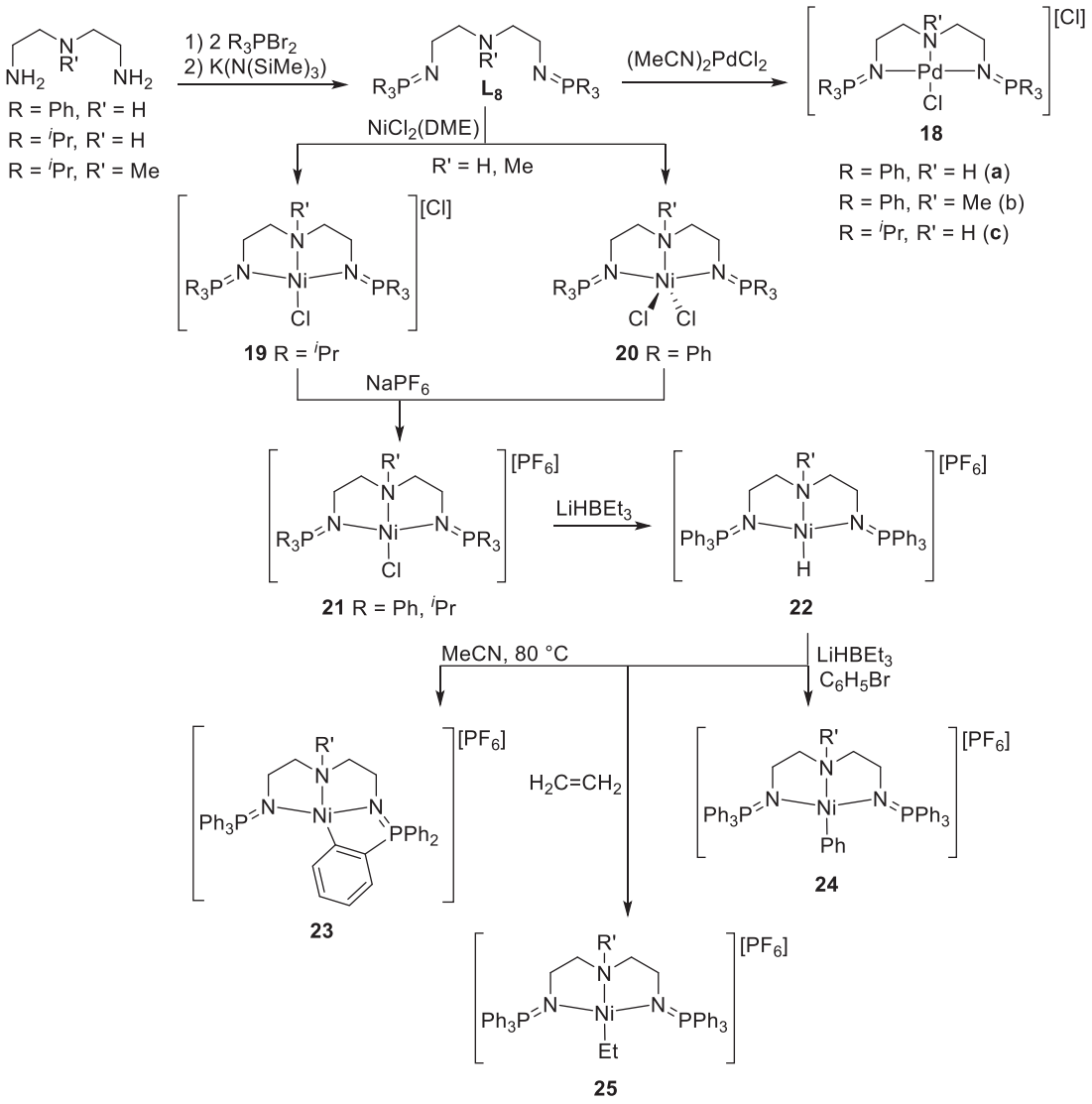

Scheme 9 Synthesis of palladium complexes **18** and reaction chemistry of nickel complexes **19**–**22**.[31,32]

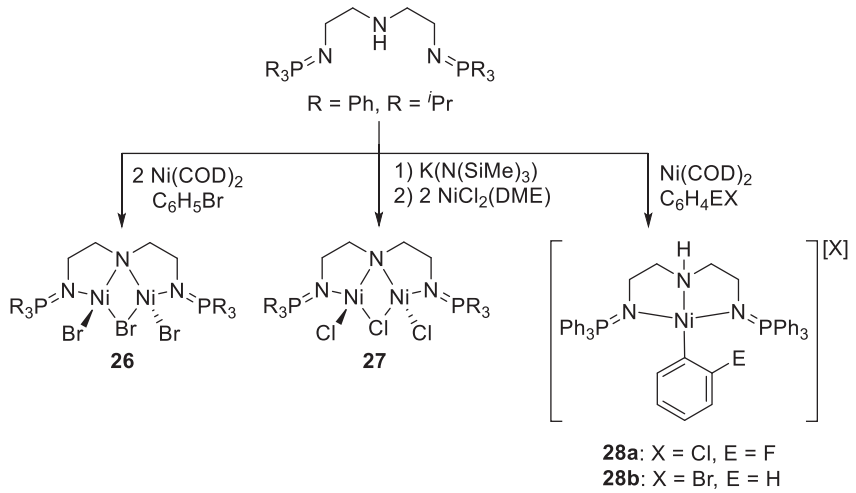

Scheme 10 Synthesis of dinuclear nickel complexes **26**–**28**.[31,32]

The Wang group synthesized the asymmetric *endo* ligand, 2-($Me_3SiN{=}PPh_2$)-6-($Me_3SiN{=}PPh_2CH_2$)C_5H_3N, $\mathbf{L_9}$, from which they produced the di- and monoethyl species of aluminium, (2-($Me_3SiN{=}PPh_2$)-6-($Me_3SiN{-}PPh_2{=}CH$)C_5H_3N)$AlEt_2$, **29**, and zinc, (2-($Me_3SiN{=}PPh_2$)-6-($Me_3SiN{-}PPh_2{=}CH$)C_5H_3N)ZnEt, **30**, respectively (Scheme 11).[33] Both species are 4-coordinate with the ligand bound in a κ^2 coordination mode to the aluminium center in **29** and κ^3 to zinc in complex **30**. These complexes were evaluated for their ability to catalyze the ring-opening polymerization of ε-caprolactone, with both exhibiting moderate activity and generating high molecular weight polymer ($M_n = 174{,}000$ g mol^{-1} (**29**) and 37,500 g mol^{-1} (**30**)) at elevated temperature.

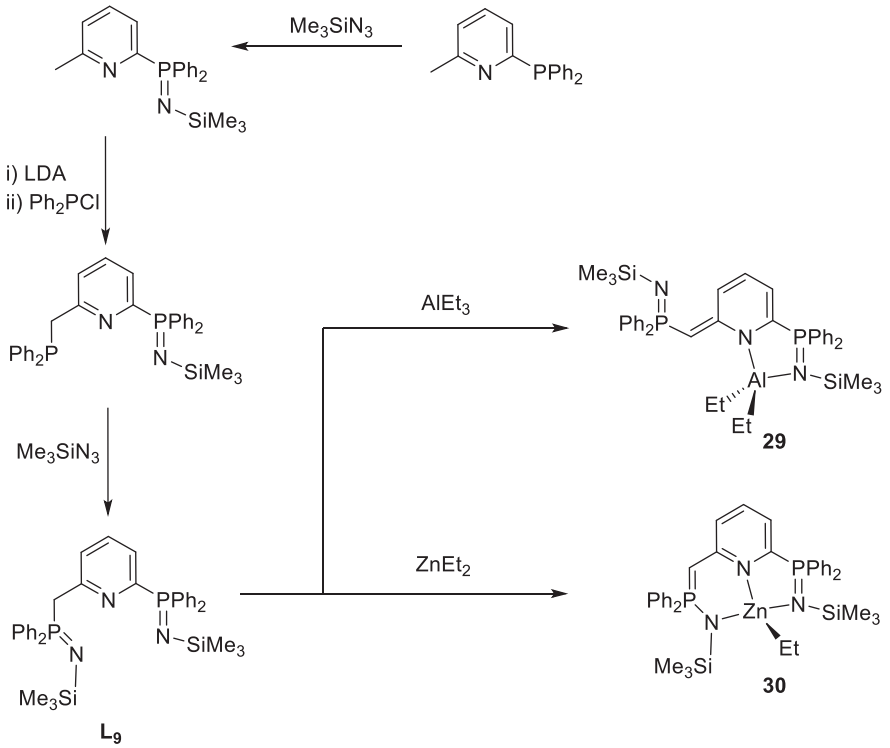

Scheme 11 Synthesis of the asymmetric bisphosphinimine ligand $\mathbf{L_9}$ and corresponding metal ethyl species **29** and **30**.[33]

The related asymmetric *NNN*-ligand 1-($PhN{=}PPh_2$)-2-($NC(Ph){=}C(H)P^iPr_2{=}NPh$)$C_6H_4$, $\mathbf{L_{10}}$, proved useful for supporting nickel chloride, $\mathbf{L_{10}}$NiCl, **31**, and butyl, $\mathbf{L_{10}}Ni^nBu$, **32**, complexes that are effective catalysts for Negishi and Kumada cross-coupling reactions (Scheme 12).[34,35] Complex **31** was particularly efficient at cross-coupling a large variety of substituted aryl chlorides.[35] Notably, catalyst loadings as low as 0.005 mol% of **31** and **32** could be used for coupling monosubstituted aryl iodides and chlorides with aryl Grignard reagents.[34]

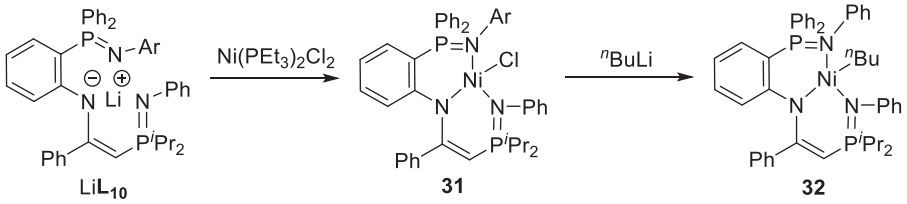

Scheme 12 Synthesis of nickel cross-coupling catalysts **31** and **32**.[34,35]

A large library of bidentate *exo* ligands that feature aliphatic and aromatic backbones, $\mathbf{L_{11}}$, were reported by Alt and used to create a series of nickel bromide complexes, $\mathbf{L_{11}}NiBr_2$, **33a-n** (Scheme 13).[36] These species were found to catalyze the dimerization of propene following activation with 2 equivalents of PPh_3 and methylaluminoxane (MAO, Al/Ni = 500). Several of the members of this family of complex, especially those bearing electron withdrawing backbone substituents or featuring delocalized π-electrons, demonstrated extremely high activity for this transformation. Notably, **33l**, which is supported by a ligand that possesses all such properties, as well as the largest bite angle of the studied nickel complexes, afforded the highest activity (918,362 g polymer/mol(cat.)*h).[36] Dimerization gave several branched alkenes with moderate selectivity for the desired product, 2,3-dimethylbut-1-ene (DMB-1). The addition of bulky alkyl phosphines (e.g. PCy_3, P^iPr_3, MeP^tBu_2), as opposed to PPh_3, greatly increased the proportion of DMB-1 and 2-methylpent-1-ene (MP-1). Lower reaction temperatures also favored DMB-1 and MP-1.[36]

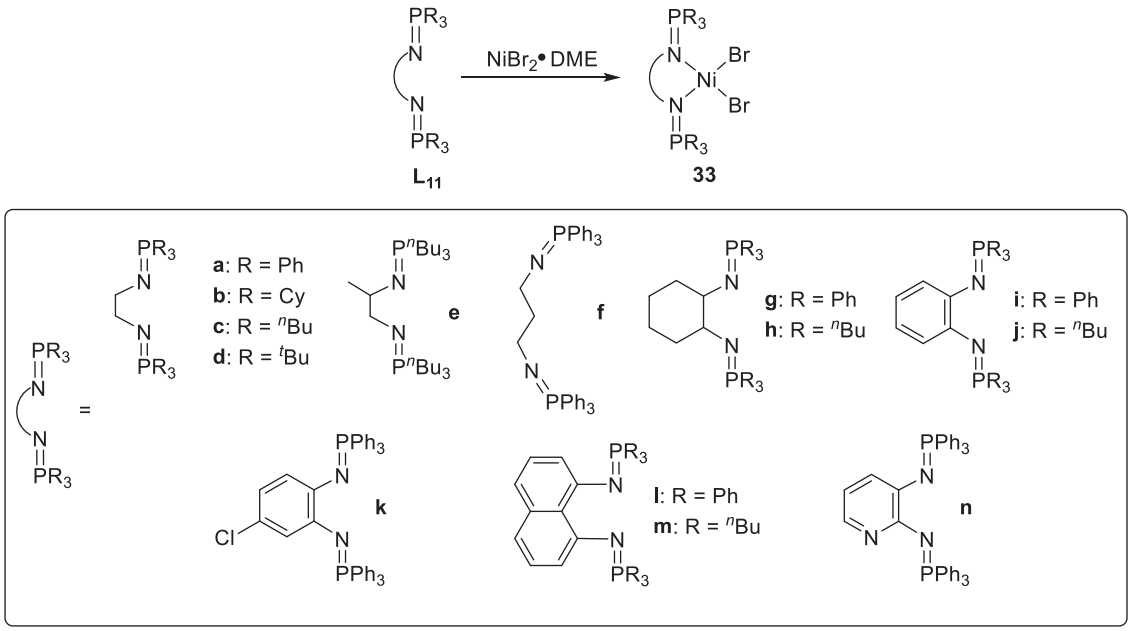

Scheme 13 Synthesis of nickel bromide complexes **33**.[36]

Utilizing the *exo* ligand 2,6-$(CH_2N{=}PPh_3)_2C_5H_3N$, $\mathbf{L_{12}}$, Auffrant and Cheisson prepared an array of copper complexes,[37] including the asymmetric, dinuclear cationic species, $[\mathbf{L_{12}}]_2Cu_2[PF_6]_2$, **34** (Scheme 14). The coordination spheres of the two metal centers in this complex differ substantially from each another, with one approaching linearity (N–Cu–*N* = 173.7 (1)°) and the other exhibiting distorted tetrahedral geometry. Addition of excess PEt_3 to **34** yielded the mononuclear $[NN\text{-}\mathbf{L_{12}}CuPEt_3][PF_6]$, **35**, which contains a free phosphinimine moiety, as the supporting ligand coordinates to copper by a κ^2 bonding mode. The complex *NN*-$\mathbf{L_{12}}$CuBr, **36**, which can be prepared by straightforward addition of $\mathbf{L_{12}}$ to several Cu^I bromide sources, also features an uncoordinated phosphinimine; low

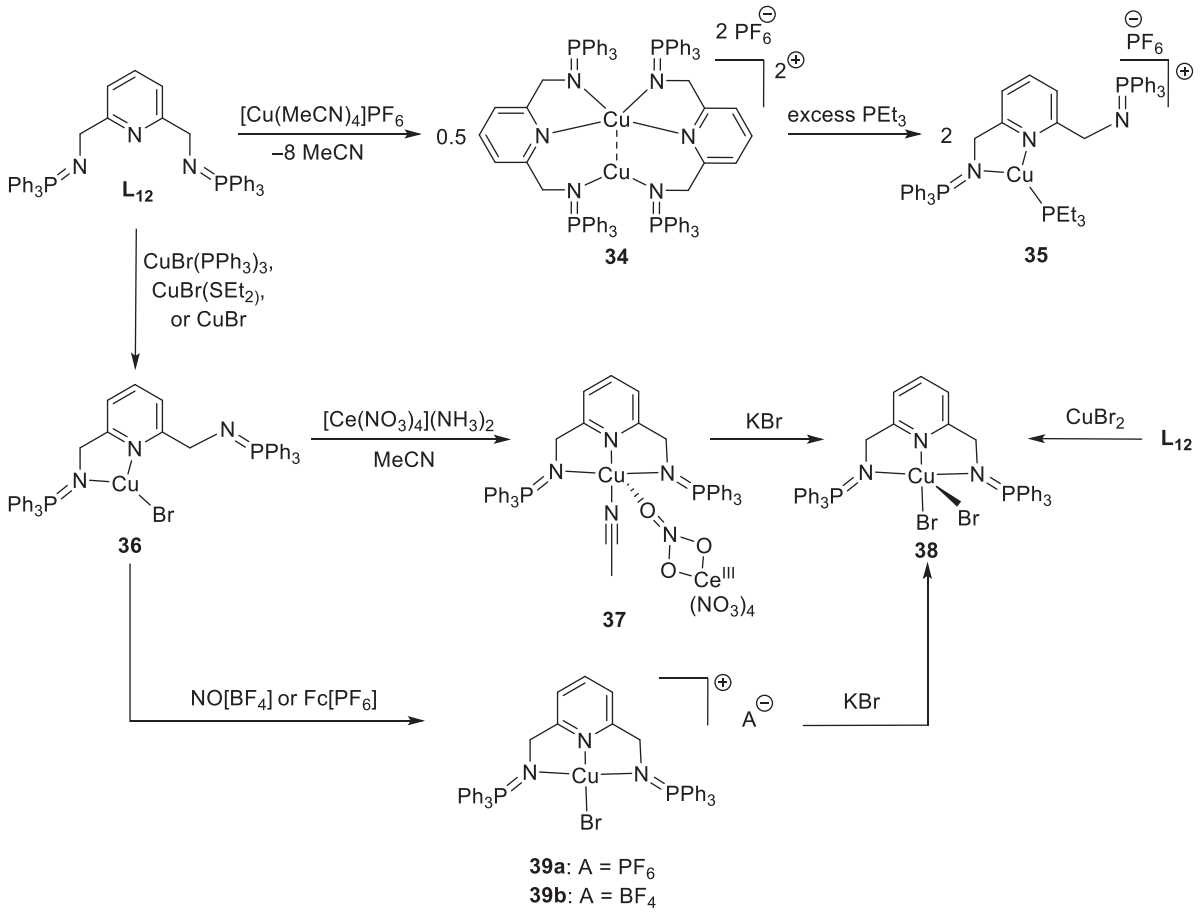

Scheme 14 Synthesis of copper complexes **34**–**39**.[37]

temperature NMR experiments revealed the two phosphinimine donors to be exchanging in solution.[37] The cationic species, $\mathbf{L_{12}}Cu(NCMe)O{=}NO_2Ce(III)(NO_3)_4$, **37**, and $[\mathbf{L_{12}}CuBr][A]$, **39a**: A = PF_6; **39b**: A = BF_4, were accessible via the addition of $[Ce(NO_3)_4](NH_3)_2$/MeCN and fluoride salts to **36**, respectively. Subsequent addition of KBr to dinuclear **37** gave the Cu^{II} complex, $\mathbf{L_{12}}CuBr_2$, **38**. Complex **38** was also generated by reaction of $CuBr_2$ and $\mathbf{L_{12}}$, as well as by combining KBr with complex **39**. Complexes **34** and **35** catalyze the cyclopropanation of styrene with ethyldiazoacetate ($N{=}N{=}CH{-}CO_2Et$), heavily favoring the *cis* cyclopropane product. Both complexes also mediate the [3 + 2] cycloaddition of phenylacetylene and 4-methoxybenylazide.[37]

The pyrrole-based bisphosphinimine pincer ligand 2,5-$(4\text{-}^{i}PrC_6H_4N{=}PR_2)_2C_4H_2NH$, $\mathbf{L_{13}}$, has been successfully utilized to support a family of rhodium complexes that engage in various reactions with small molecules. For example, reaction of $\mathbf{L_{13Ph}}Rh(COE)$, **40a**, with H_2 gas liberates cyclooctane (COA) and affords an asymmetric dinuclear species $H_2\mathbf{L_{13Ph}}Rh_2$, **40b**, which contains one equivalent of H_2 as a bridging hydride (H^-) and protonated (H^+) phosphinimine (Scheme 15).[38] Although addition of cyclooctene to complex **40b** does not regenerate **40a**, addition of the smaller alkene, ethylene, affords $\mathbf{L_{13Ph}}Rh(H_2C{=}CH_2)$, **40c**. Both complexes **40a** and **40c** serve as alkene and alkyne hydrogenation catalysts; **40b** was determined to be the catalyst resting state

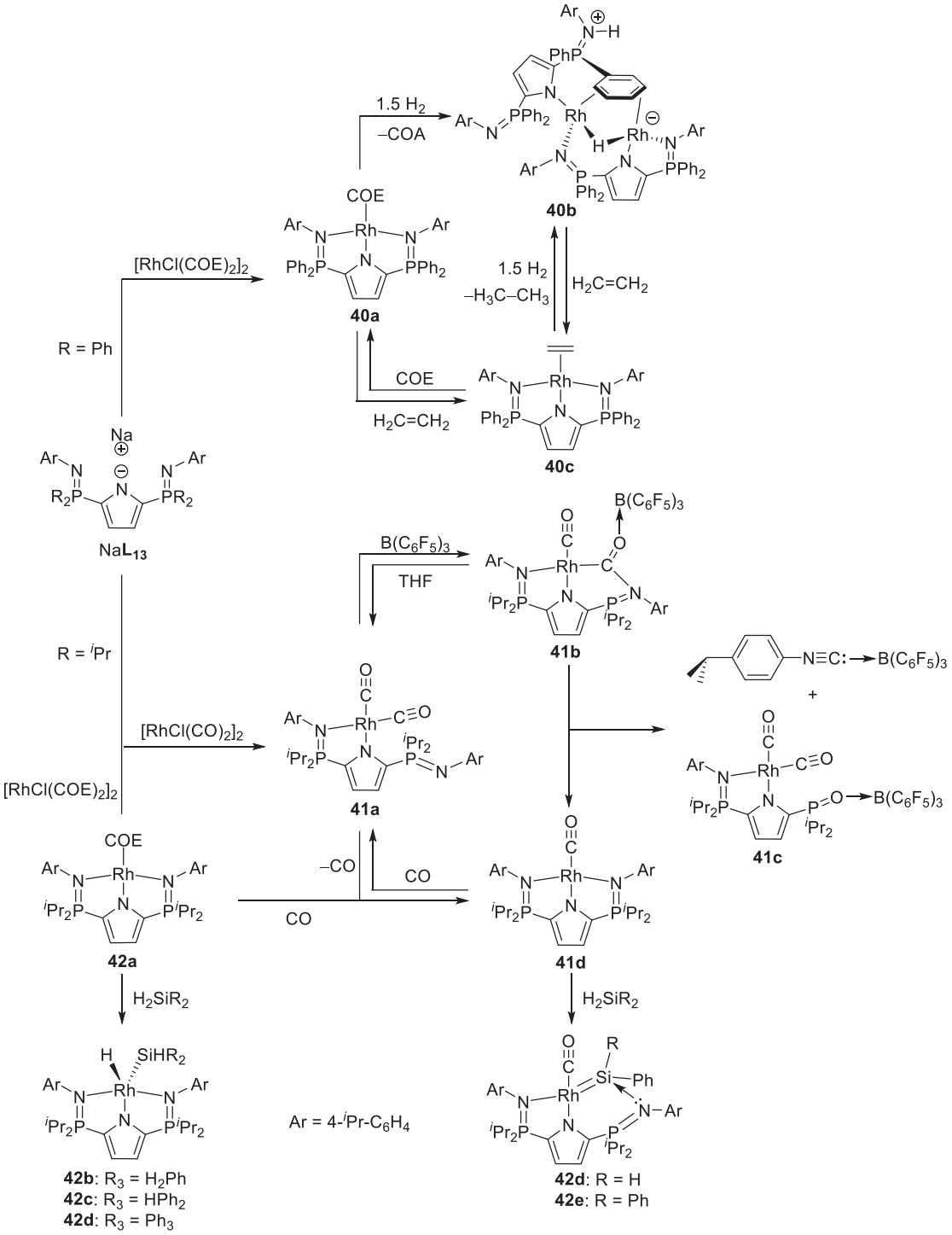

Scheme 15 Synthesis and reaction chemistry of rhodium complexes supported by the bisphosphinimine pyrrole-based ligand $\mathbf{L_{13}}$.[38–40]

once all of the H_2 and/or substrate has been consumed. Notably, when diphenylacetylene is hydrogenated *trans*-stilbene is the sole alkene product. If more forcing conditions are employed diphenylethane can be obtained.

Upon replacement of the P–Ph substituents in $\mathbf{L_{13Ph}}$ with ^{i}Pr groups further metal ligand cooperative activation of small molecules was observed. For example, when $\mathbf{L_{13iPr}}Rh(CO)_2$, **41a**, is exposed to one equivalent of $B(C_6F_5)_3$, the unusual encounter complex *NN*-$\mathbf{L_{13iPr}}Rh(CO)_2B(C_6F_5)_3$, **41b**, wherein one CO ligand is bonded to rhodium, a phosphinimine nitrogen and boron, was isolated (Scheme 15). Although the O→B interaction is weak and can be cleaved upon addition of THF, over time in solution complete C≡≡O bond scission occurs, ultimately generating half an equivalent of each *NN*-$\mathbf{L_{13iPr}}Rh(CO)_2P{=}O{-}B(C_6F_5)_3$, **41c**, the monocarbonyl $\mathbf{L_{13iPr}}RhCO$, **41d**, and the borane-capped isocyanide 4-^{i}Pr$C_6H_4N{\equiv}C{\rightarrow}B(C_6F_5)_3$.[39] When the cyclooctene adduct $\mathbf{L_{13iPr}}Rh(COE)$, **42a**, was reacted with silanes, conventional Si–H oxidative addition provided the five-coordinate silyl hydride species $\mathbf{L_{13iPr}}Rh(H)SiR_3$, **42b**: $R_3 = H_2Ph$; **42c**: $R_3 = HPh_2$; **42d**: $R_3 = Ph_3$.[40] Conversely, reaction of $\mathbf{L_{13iPr}}RhCO$ with $PhSiH_3$ or Ph_2SiH_2 afforded the corresponding base-stabilized silylenes $\mathbf{L_{13iPr}}Rh{=}SiPhR(CO)$, **42e**: R = H; **42f**: R = Ph, via an unusual dehydrogenative process.[40]

1.07.2.3.2 Lanthanide and actinide metals

Cui and co-workers developed an *endo* ligand that resembles the amine containing frameworks reported by Stephan, $HN(RN{=}PPh_2)_2$, $\mathbf{L_{14}}$, though lacking the organic linkers between the anionic nitrogen and the two flanking phosphinimines.[41–43] With this scaffold a wide variety (e.g. dialkyl, alkyl/amido, hydride, imido) of complexes of scandium ($\mathbf{L_{14}}Sc(CH_2SiMe_3)_2$, **43a**, $\mathbf{L_{14Ph}}Sc(CH_2SiMe_3)NHDipp$, **48**, $\mathbf{L_{14Ph}}Sc{=}NDipp(DMAP)_2$, **49**[41]) yttrium, ($\mathbf{L_{14}}Y(CH_2SiMe_3)_2$, **43b**, $\mathbf{L_{14Dipp}}Y(Et)AlEt_4$, **45**, $\mathbf{L_{14Dipp}}Y(Me)AlMe_4$, **46**, $\mathbf{L_{14Dipp}}Y(CH_2SiMe_3)NHDipp$, **47a**, $[\mathbf{L_{14Dipp}}YH_2]_2$, **50a**, $[\mathbf{L_{14Dipp}}Y]_2H_3(THF)_2$, **51**[42,44]) lutetium, ($\mathbf{L_{14}}Lu(CH_2SiMe_3)_2$, **43c**, $\mathbf{L_{14Dipp}}Lu(CH_2SiMe_3)NHDipp$, **47b**, $[\mathbf{L_{14Dipp}}LuH_2]_2$, **50b**), and neodymium ($L_{14Ph}Nd(BH_4)_2(THF)_2$, **44**) were prepared (Schemes 16 and 17).[43] Amongst these diverse

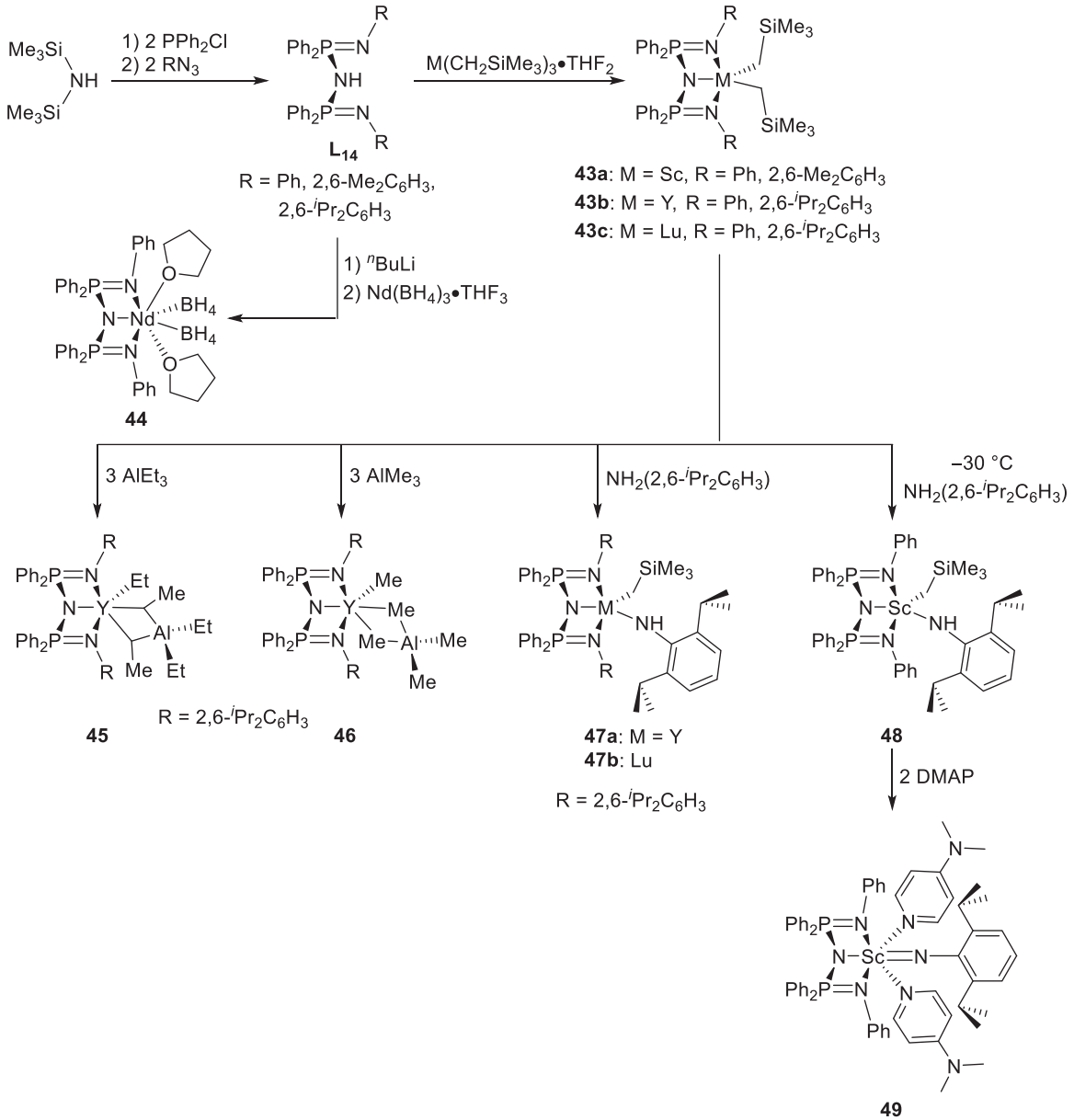

Scheme 16 Synthesis of rare earth metal complexes **43–49**.[41–43]

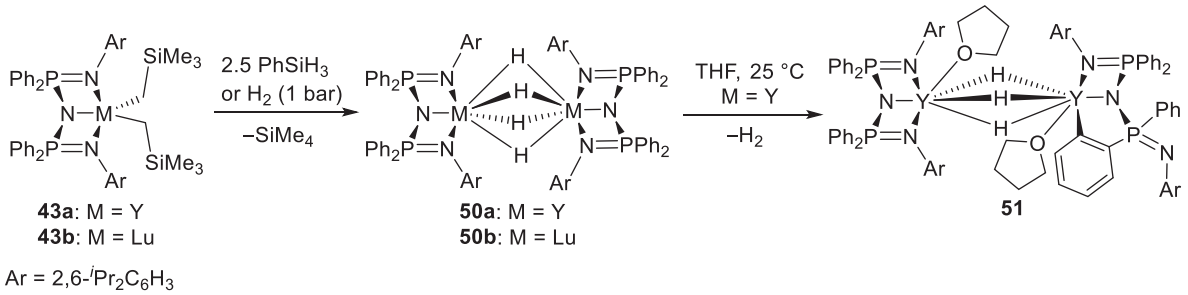

Scheme 17 Synthesis and cyclometalative decomposition of dinuclear tetrahydride yttrium and lutetium complexes **50a** and **50b**.[44]

complexes, perhaps the most noteworthy is the rare terminal scandium imide $\mathbf{L_{14Ph}}Sc{=}NDipp(DMAP)_2$, **49**, which was generated by reaction of the precursor alkyl/amide $\mathbf{L_{14Ph}}Sc(CH_2SiMe_3)NHDipp$, **48**, with two equivalents of 4-dimethylaminopyridine. It should also be noted that while most of these complexes were thermally stable under ambient conditions, the dinuclear tetrahydride species $[\mathbf{L_{14Dipp}}YH_2]_2$, formed by addition of either 2.5 equivalents of $PhSiH_3$ or 1 atm of H_2 gas to **43a**, was prone to PPh cyclometalation at 25 °C in THF (Scheme 17).[44]

Complexes $\mathbf{L_{14Xyl}}Sc(CH_2SiMe_3)_2$, $\mathbf{L_{14Dipp}}Y(CH_2SiMe_3)_2$ and $\mathbf{L_{14Dipp}}Lu(CH_2SiMe_3)_2$, which showcase sterically demanding xylyl and Dipp substituents, were found to be inactive toward isoprene polymerization,[43] whereas the smaller species $\mathbf{L_{14Ph}}M(CH_2SiMe_3)_2$ (M = Sc, Y, Lu), upon activation with $[CPh_3][B(C_6F_5)_4]$ and 10 equivalents of Al^iBu_3, completely polymerized 1000 equivalents of isoprene after 5 h at 25 °C in toluene solution. Increasing the metal size resulted in decreased *trans*-1,4-selectivity (Sc = 90.0%, Lu = 76.3%, Y = 54.3%) due to the greater availability of the η^4 coordination mode for isoprene.

In addition to the previously discussed pyrrole-based bisphosphinimine ligand $\mathbf{L_{13}}$,[38–40] Hayes and colleagues also reported the carbazole analogue 1,8-$(ArN{=}PR_2)_2$-3,6-dimethylcarbazole, $\mathbf{L_{15}}$ (Fig. 3).[45–53] Unlike its pyrrole brethren, construction of an *NNN*-pincer scaffold required additional steps, as substitution at the 3 and 6 positions of carbazole is preferred. Another notable difference between the two scaffolds is that upon coordination to a metal $\mathbf{L_{15}}$ froms 6-membered chelate rings, as opposed to 5-membered rings when $\mathbf{L_{13}}$ is employed. This necessarily places the phosphorus and nitrogen substiuents in closer proximity to the metal center. The consequence of such steric crowding can prove beneficial, as it protects the metal center, but can also lead to decomposition by intramolecular bond activation processes (vide infra).

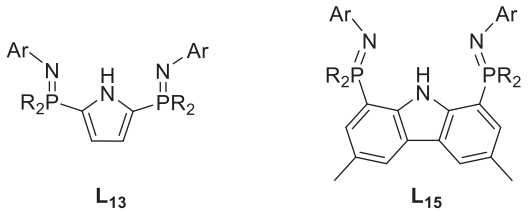

Fig. 3 General structures of Hayes' *NNN*-pincer ligands $\mathbf{L_{13}}$ and $\mathbf{L_{15}}$.[45–53]

Using derivatives of $\mathbf{L_{15}}$ a broad array of scandium, yttrium and lutetium complexes have been prepared by alkane elimination and salt metathesis routes.[45–50] Many of these species were prone to one or two cyclometalation reactions with the nitrogen and phosphorous substituents.[45–49] For example, $\mathbf{L_{15Ph}}M(CH_2SiMe_3)_2$, **52a**: M = Lu; **53a**: M = Y, underwent double PPh cyclometalation to liberate two equivalents of $SiMe_4$ and *NNNCC*-$\mathbf{L_{15Ph}}$*MTHF **52b**: M = Lu; **53b**: M = Y. Unlike many cyclometalated complexes, **52b** readily reacts with amines to regenerate the PPh groups and provide access to either the diamido species $\mathbf{L_{15Ph}}Lu(NHAr')_2$, **52c**, (Ar′ = Mes or 2,4,6-$^iPr_3C_6H_2$), or upon treatment with the more bulky amine 2,4,6-$^tBu_3C_6H_2NH_2$ (Mes*), the monoamido monocyclometalated complex *NNNC*-$\mathbf{L_{15Ph}}$*LuNHMes*, **52d**.[50] Further heating converted the PPh cyclometalated **52d** into the NAr cyclometalated complex *NNNC*-$\mathbf{L_{15*Ph}}$LuNHMes*, **52e** (Scheme 18A).

Attempts to restrict PPh bond activation by replacing the phenyl groups with a phospholane ring were unsuccessful; each phospholane in $\mathbf{L_{15Pipp,C4H8}}Sc(CH_2SiMe_3)_2$, **54a**, participated in cyclometalation, giving rise to *NNNCC*-$\mathbf{L_{15Pipp,C4H8}}$*Sc, **54b**. Although the lutetium analogue $\mathbf{L_{15Pipp,C4H8}}Lu(CH_2SiMe_3)_2$, **55a**, proved inert to phospholane cyclometalation, over the course of 3 h at 296 K in benzene one of the 4-$^iPrC_6H_4$ nitrogen groups underwent *ortho* C–H activation to produce $\mathbf{L_{15Pipp*,C4H8}}LuCH_2SiMe_3$, **55b**.[49] Similarly, when PMe_2 groups were incorporated into $\mathbf{L_{15}}$, rapid PMe cyclometalation was observed in aromatic solvents (Scheme 18B).[49]

Upon replacement of the aryl substituents on nitrogen with pyrimidine, which lacks ortho C–H groups, CH_2SiMe_3 migration from lutetium to pyrimidine in $\mathbf{L_{15Pm,Ph}}Lu(CH_2SiMe_3)_2$, **56a**, afforded the asymmetric dinuclear complex $[\mathbf{L_{15Pm*,Ph}}Lu]_2(THF)$, **56b**, wherein all four pyrimidine rings have been dearomatized.[46] Other efforts to avoid C–H bond activation included the

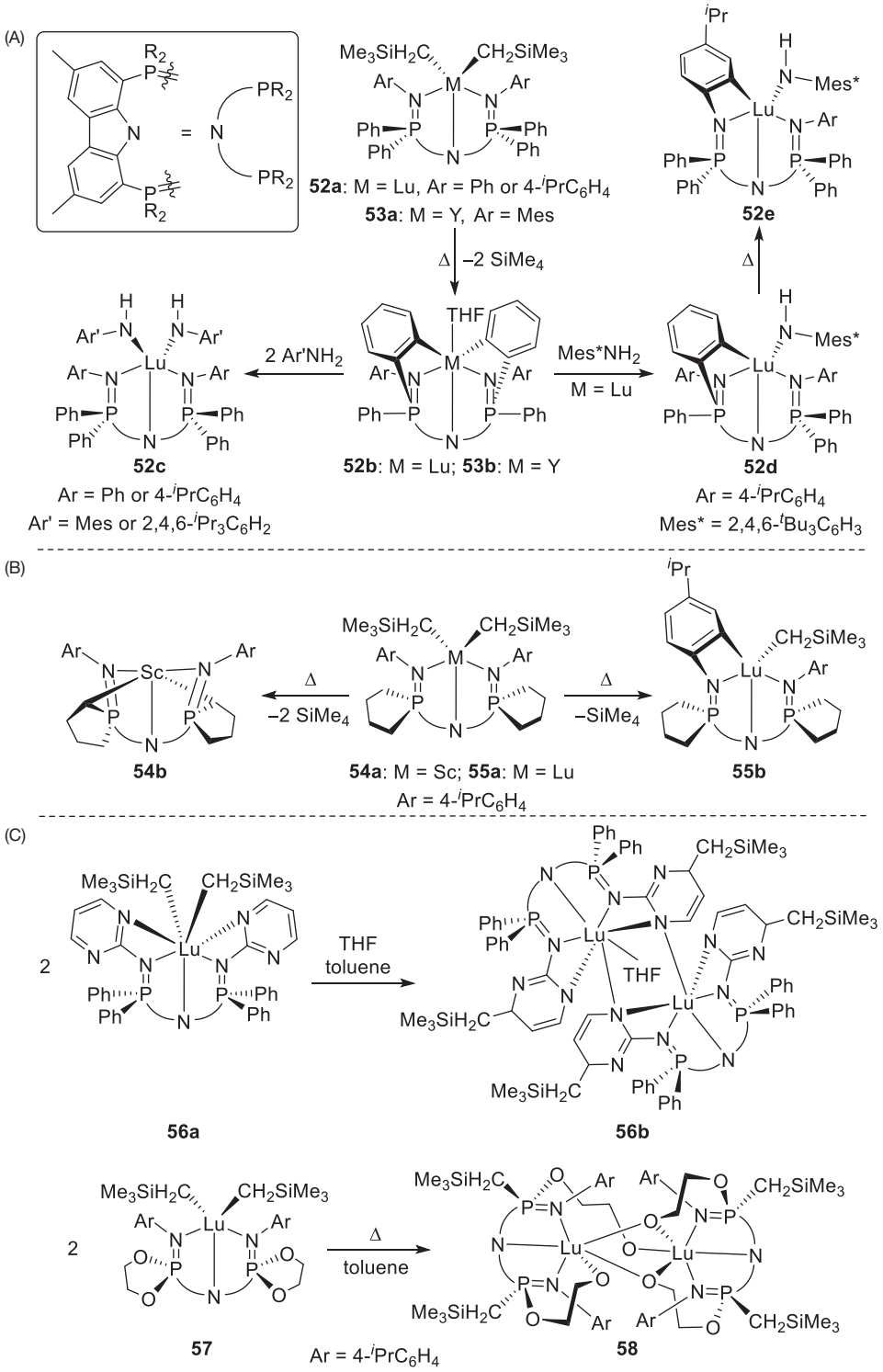

Scheme 18 (A) Synthesis and cyclometallation of yttrium and lutetium complexes **52a** and **53a**; (B) Phospholane and NAryl cyclometallation in scandium and lutetium complexes **54a** and **55a**; (C) Formation of dinuclear lutetium species **56b** and **58** via CH_2SiMe_3 migration from lutetium to pyrimidine and dioxaphospholane groups.[45–50]

installation of dioxaphospholane moieties. Unfortunately, the lutetium species $\mathbf{L_{15Pipp,O2C2H4}}Lu(CH_2SiMe_3)_2$, **57**, suffered from facile alkyl group transfer to phosphorus, along with simultaneous cleavage of the phosphonimidate ester P–O bonds, ultimately yielding [*NNNOO*-$\mathbf{L_{15Pipp,O2C2H4*}}$Lu]$_2$, **58** (Scheme 18C).[47]

When $\mathbf{L_{13}}$ was used the corresponding rare earth dialkyl species $\mathbf{L_{13Ph}}Ln(CH_2SiMe_3)_2$, **59a**: Ln = Sc; **59b**: Ln = Y; **59c**: Ln = Er; **59d**: Ln = Lu, all of which are monomeric and free of Lewis bases, proved far more stable than those supported by the carbazole-based ligand $\mathbf{L_{15}}$ (vide supra).[51–53] In fact, no degradation was observed even after 4.5 h at 60 °C in solution (Scheme 19A). Upon changing the metal to the larger samarium, it was not possible to isolate, or even observe, the putative dialkyl species $\mathbf{L_{13Ph}}Sm(CH_2SiMe_3)_2$, **59e**. Instead, the singly NAryl metalated species *NNNC*-$\mathbf{L_{13*Ph}}SmCH_2SiMe_3(THF)$, **60**, was obtained.[52] Complex **60**, upon exposure to a second equivalent of $\mathbf{L_{13}}$ gives rise to the doubly ligated ($\mathbf{L_{13Ph}}$)*NNNC*-$\mathbf{L_{13*Ph}}$Sm, **61**. In the absence of excess ligand complex **60** proceeds to undergo multiple intra- and intermolecular C–H activations, eventually generating [*NNNCCC*-$\mathbf{L_{13Ph}}$Sm]$_2$, **62** (Scheme 19B).[52]

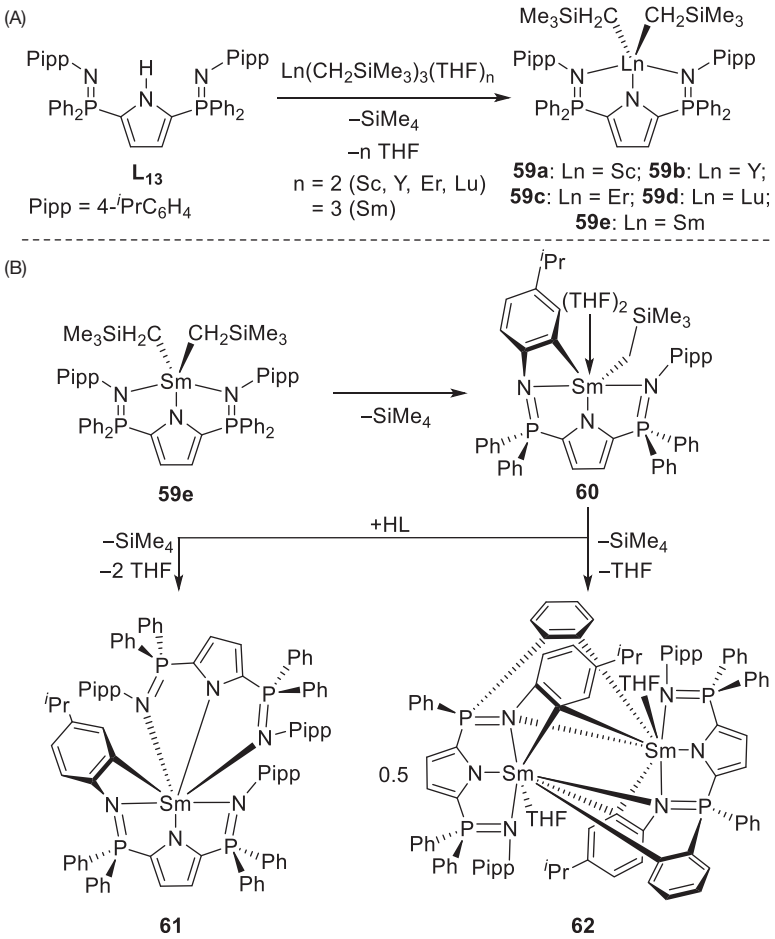

Scheme 19 (A) Synthesis of thermally stable rare earth complexes using the pyrrole-based ligand $\mathbf{L_{13}}$; (B) decomposition of samarium complex **59c** via cyclometallation.[51–53]

Given the well-behaved nature of complex **59d**, attempts were made to synthesize a lutetium imide. The mixed alkyl/amido imide precursor $\mathbf{L_{13Ph}}LuCH_2SiMe_3(NHCPh_3)$, **63a**, was prepared by reaction of complex **59d** with one equivalent of the sterically demanding amine Ph_3CNH_2.[53] Although $SiMe_4$ loss was observed after heating at 80 °C, the product was the trityl-metalated complex $\mathbf{L_{13Ph}}Lu(NC\text{-}NHCPh_3)$, **63b**, as opposed to the desired imide $\mathbf{L_{13Ph}}Lu{=}NCPh_3$. Additional heating led to half an equivalent of $\mathbf{L_{13Ph}}Lu(NHCPh_3)_2$, **63c**, which can be independently synthesized by the reaction of **63a** with Ph_3CNH_2, as well as a myriad of unidentified products. Notably, when the Lewis base 4-dimethylaminopyridine (DMAP) was added to **63a**, a similar product mixture was obtained, though no spectroscopic evidence for the formation of intermediate **63b** was observed (Scheme 20).[53]

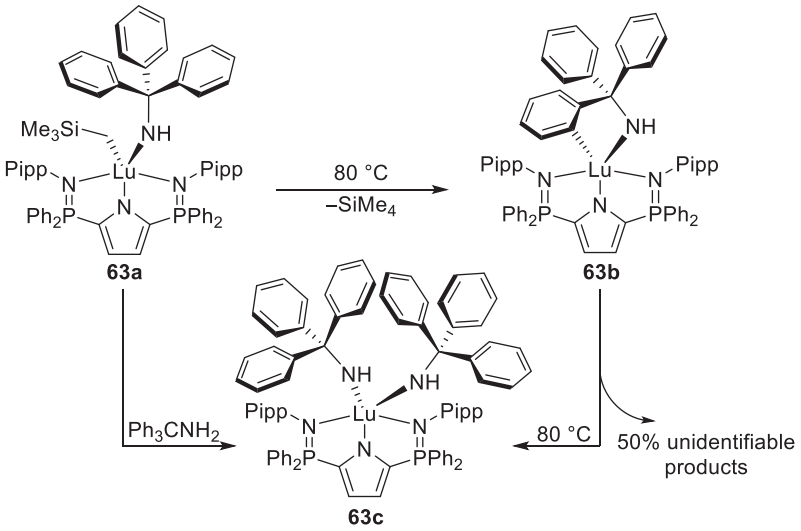

Scheme 20 Decomposition of alkyl/amido complex **63a**.[53]

A study into the coordination modes of Cp* (C_5Me_5) and Tmp (C_4PMe_4) ligands bound to ytterbium and supported by *exo* pincer ligands, 2,6-$(CH_2N{=}PR_3)_2C_5H_3N$, $\mathbf{L_{12R}}$, R = Ph, Cy, Et, revealed both κ^2 and κ^3 bonding modes are viable in these systems.[54] The steric bulk provided by the phosphorus substituents dictated whether κ^2 or κ^3 bonding was observed. Complexes bearing Cp* ligands, *NN*-$\mathbf{L_{12R}}$YbCp*, **64a**: R = Et; **64b**: R = Ph, exhibited phosphinimine exchange, while the bulkier cyclohexyl-substituted ligand $\mathbf{L_{12Cy}}$ did not react with Cp*$_2$Yb●THF (Scheme 21). Complexes $\mathbf{L_{12R}}$Yb(Tmp)$_2$, **66a**: R = Et; **66b**: R = Cy, wherein $\mathbf{L_{12R}}$ is κ^3 bound, contain Tmp ligands that are rapidly exchanging between η^5 and η^1 bonding modes. Conversely, when R = Ph, *NN*-$\mathbf{L_{12Ph}}$Yb(Tmp)$_2$, **65**, $\mathbf{L_{12Ph}}$ is κ^2 bound and both Tmp ligands are coordinated in an η^5 fashion.[54]

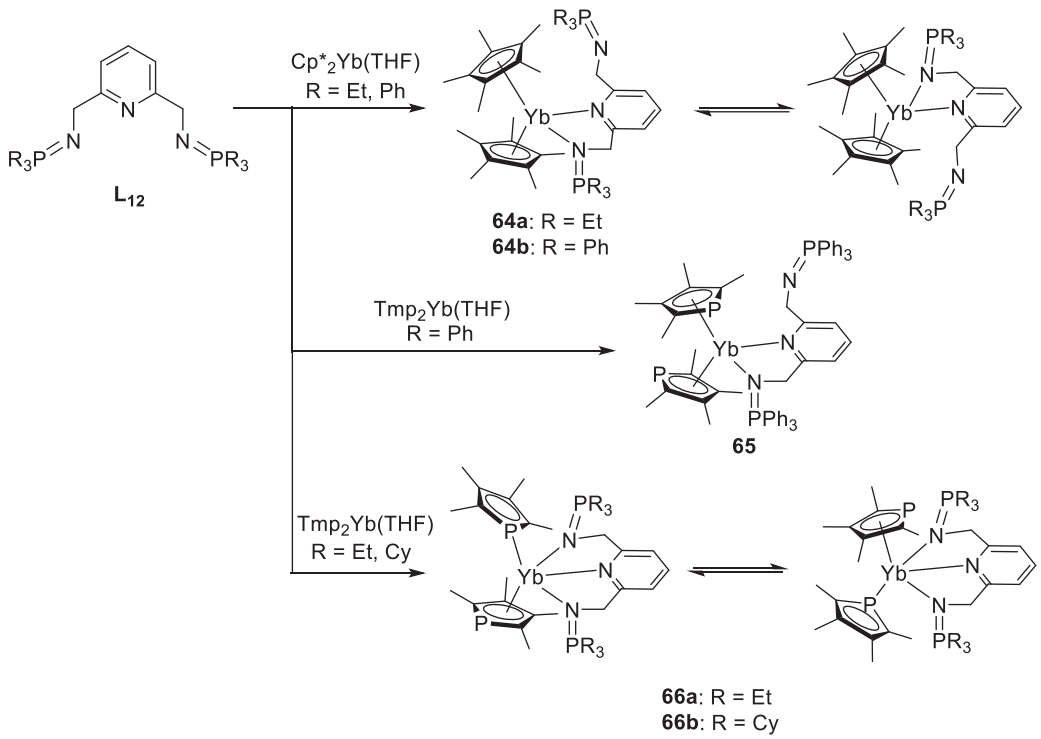

Scheme 21 Ligand fluxionality in ytterbium complexes **64–66**.[54]

The same bisphosphinimine ligand was used by Auffrant et al. to stabilize several low valent *f*-block iodide complexes, including the six coordinate species $\mathbf{L_{12}}UI_3$, **67**, $\mathbf{L_{12}}YbI_2THF$, **68a**, and $\mathbf{L_{12}}SmI_2THF$, **68b** (Scheme 22).[55] In this work, the ligand backbone proved to be redox-active; an unusual example of a rare-earth charge-separated ketyl radical, $\mathbf{L_{12Ph}}YbI_2OC\bullet Ph_2$, **69**, was prepared by reaction of complex **68a** with benzophenone. In addition, ligand-based radical coupling resulted in C–C bond formation and generation of the dimeric thulium compound, $[\mathbf{L_{12*Cy}}TmI_2(THF)_2]_2$, **70**.

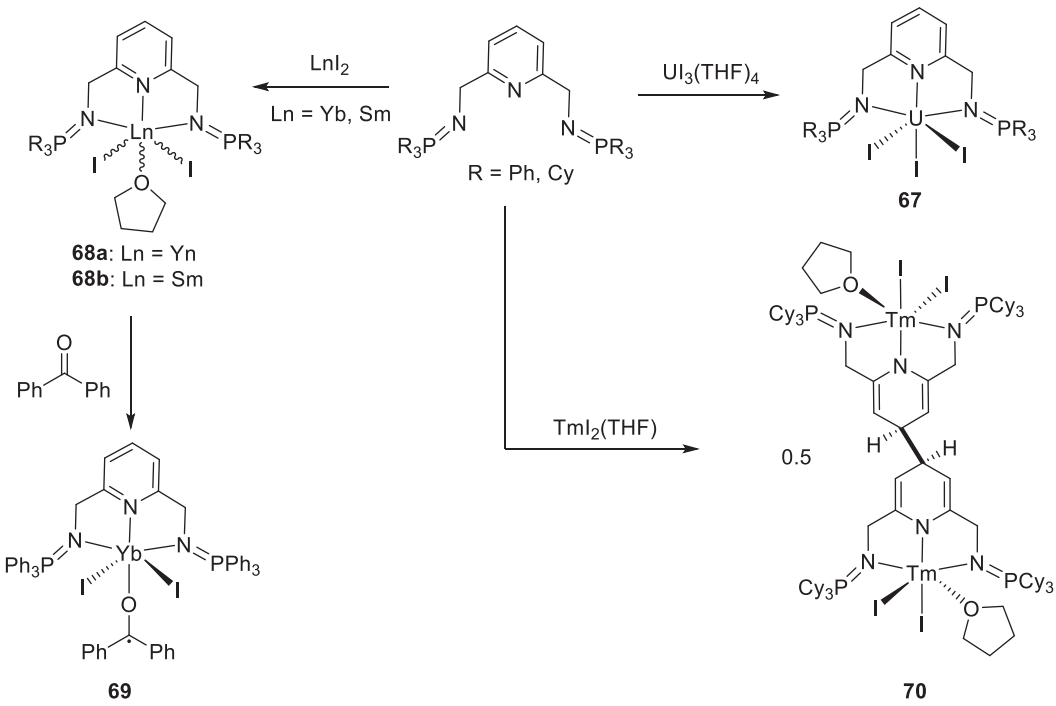

Scheme 22 Synthesis and redox activity of low-valent *f*-block iodide complexes **67** and **68**.[55]

Wang and Chai made use of $\mathbf{L_9}$ and an asymmetric analogue, 2-($Me_3SiN{=}PPh_2$)-6-(4-$MeC_6H_4N{=}PPh_2CH_2$)C_5H_3N, $\mathbf{L_{16}}$, to support complexes of ytterbium ($\mathbf{L_9}YbCH_2SiMe_3$, **71**) tin (NN-$\mathbf{L_{16}}SnCH_2SiMe_3$, **72**, and $[CCN$-$\mathbf{L_9}Sn]_2$, **73a**) and lead ($[CCN$-$\mathbf{L_9}Pb]_2$, **73b**) by treatment with the appropriate metal bis(trimethylsilyl)amide (Scheme 23).[56] Complex **71** featured the expected

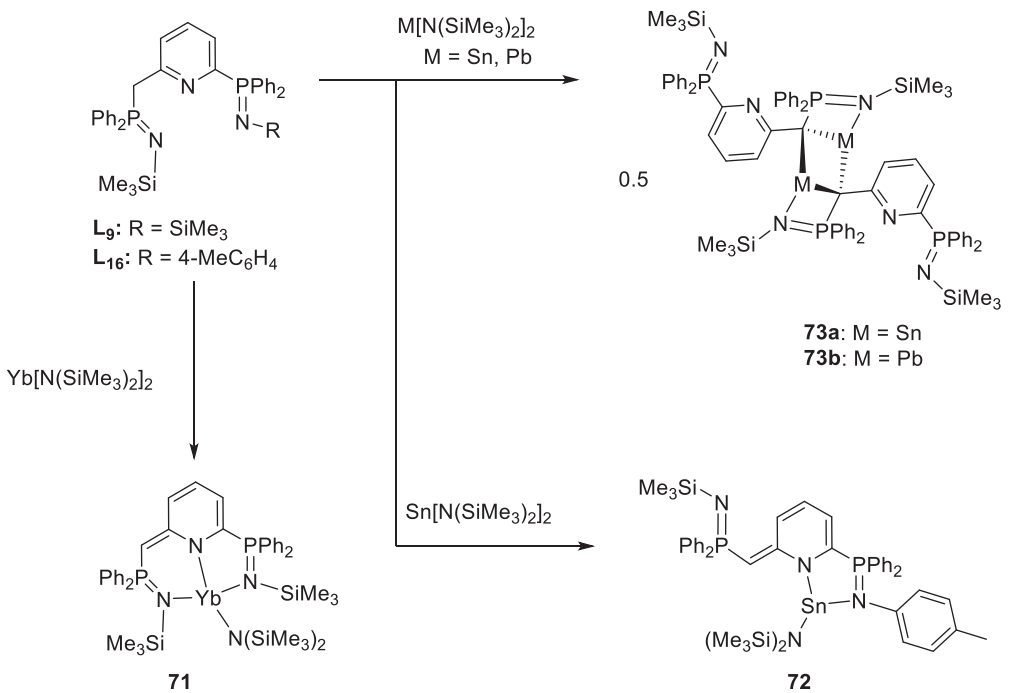

Scheme 23 Synthesis of complexes of ytterbium (**71**), tin (**72** and **73a**) and lead (**73b**).[56]

κ^3 coordination mode, but the tin center in complex **72**, possesses a dangling phosphinimine as $\mathbf{L_{16}}$ is bonded to the metal by only two nitrogen donors. The unusual dimeric species **73a** and **73b** were the result of double methylene C–H activation/amine elimination. The formally dianionic bisphosphinimine ligands are each bound to one metal center via a phosphinimine and the carbon adjacent to the bound phosphinimine. That same carbon also bridges to the other metal.[56] Neither the pyridines, nor the remaining phosphinimines are coordinated to either metal.

1.07.2.4 *NON*-Pincer Ligands

The Hayes group reported a neutral version of $\mathbf{L_{15}}$, wherein the carbazole backbone was replaced with dibenzofuran (dbf), 4,6-(ArN=PR_2)$_2$dibenzofuran, $\mathbf{L_{17}}$. This scaffold proved valuable for generating a large library of cationic complexes of zinc ([$\mathbf{L_{17}}$ZnE][A], **74a-e**)[57–61] and magnesium ([$\mathbf{L_{17}}$Mg^{n}Bu][A], **75**),[62] many of which exhibited high catalytic activity for the ring-opening polymerization (ROP) of lactones.[57–60] These species were prepared by treating the free ligands with a Brønsted acid, which afforded well-behaved salts that can be isolated and stored indefinitely under an inert atmosphere. Subsequent reaction with alkylzinc or magnesium reagents cleanly afforded cationic complexes via an alkane elimination process (**Scheme 24**).[63]

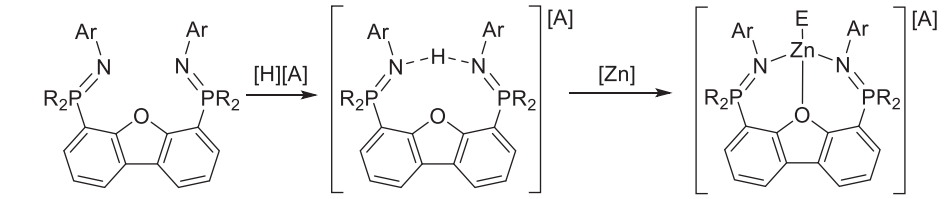

74a: R = Ph	Ar = Mes	A = $B(C_6F_5)_4$, BPh_4	E = Me, OAc, Me-(*rac*)-lactate
74b: R = Ph	Ar = 4-^{i}PrC_6H_4	A = $B[C_6H_3(m\text{-}CF_3)_2]_4$, BPh_4	E = Me
74c: R = Ph	Ar = Ph	A = $B[C_6H_3(m\text{-}CF_3)_2]_4$	E = Me-(*rac*)-lactate
74d: R = Et	Ar = CH_2Ph	A = $B[C_6H_3(m\text{-}CF_3)_2]_4$	E = Me, Me-(*rac*)-lactate
74e: R = Ph, ^{i}Pr	Ar = *m*-Xy, *p*-TrPh	A = $B[C_6H_3(m\text{-}CF_3)_2]_4$	E = Et

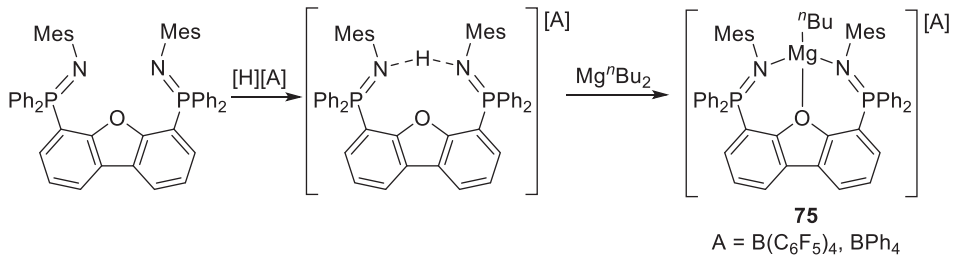

Scheme 24 Synthesis of cationic zinc and magnesium complexes **74 and 75**.[57–63]

Zinc complexes containing the methyl-(*rac*)-lactate substituent were found to be the most active for lactide polymerization, with [$\mathbf{L_{17Bn,Et}}$Zn(lactate)][B(3,5-$(CF_3)_2C_6H_3)_4$], **74d**, capable of polymerizing 200 equivalents (90% conversion) of monomer in 20 min at 25 °C.[60] In situ NMR studies revealed no induction period and first-order consumption of lactide (PDI = 1.24–1.57). Polymer analysis by NMR spectroscopy, gel permeation chromatography and MALDI-ToF mass spectrometry indicated largely atactic material with polymer chains bearing a methyl-lactate end group, suggesting a coordination-insertion mechanism. However, substantial rates of transesterification were observed. Notably, this system exhibited living characteristics; additional monomer was consumed at a similar rate more than 1 h after complete consumption of the initial quantity of lactide.

The steric hindrance provided by the ligand was found to substantially influence catalytic activity. A series of experiments aimed at tuning the steric environment at the metal center suggested that less congestion generally improved activity. The electron donating character of the ligand was similarly influential on catalyst performance; it was theorized that a more electropositive metal center would be more active, though the role played by the central oxygen donor remains unclear.[57–60] Although inert toward lactide, the magnesium complex [$\mathbf{L_{Mes}}$Mg^{n}Bu][BPh_4], **75**, exhibited extremely high activity (complete monomer consumption in 4 min at ambient temperature with a 0.77 mol% initiator loading) for the ROP of ε-caprolactone, producing relatively low PDI (<1.6) poly-(ε-caprolactone).[62]

Monophosphinimine dbf ligands, 4-(ArN=PR_2)dibenzofuran, $\mathbf{L_{18}}$, have also been used to prepare neutral and cationic zinc complexes,[64–66] and because of their similarity to their previously discussed bisphosphinimine congeners **74** and **75**, will be briefly highlighted. As with bisphosphinimine $\mathbf{L_{17}}$, the phosphinimine was introduced by deprotonating the 4-position of dibenzofuran using a strong base (^{n}BuLi) followed by reaction with a halophosphine (e.g. $ClPPh_2$). A subsequent Staudinger reaction with an aryl azide easily generated the desired achiral ligands (**Scheme 25**). The P-stereogenic variants were prepared via a more elaborate route.[66]

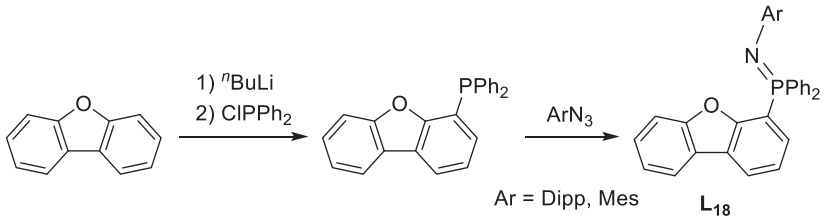

Scheme 25 Synthesis of achiral monophosphinimine ligands $\mathbf{L_{18}}$.[64–66]

Neutral four-coordinate complexes $\mathbf{L_{18Dipp}}ZnCl_2$, **77a**, $\mathbf{L_{18Mes}}Zn(C_6F_5)_2$, **77b**, and $\mathbf{L_{18Dipp}}ZnEt(OTf)$ **77c**, were made by the addition of the requisite zinc starting material to the neutral ligand (Scheme 26).[64] The cationic species $[\mathbf{L_{18Dipp}}ZnEt][A]$, **78a**: $A = B(C_6F_5)_4$; **78b**: $A = SO_3CF_3$, were synthesized according to the ligand protonation/alkane elimination protocol discussed previously.[65] In an effort to impart stereochemical control during the polymerization of lactide, the P-chiral ligands, $\mathbf{L_{18Dipp,MePh}}$ and $\mathbf{L_{18Mes,MePh}}$, and cationic zinc complexes $[\mathbf{L_{18}}ZnR][B(C_6F_5)_4]$, **80**: R = Et; **81**: R = lactate, were designed and prepared.[66] Although high activity and conversion was maintained, the resultant polymers were atactic and suffered from bimodal and broad molecular weight distributions.[65,66] Related P-stereogenic bisphosphinimine ligands $\mathbf{L_{17MePh}}$ and corresponding zinc complexes $[\mathbf{L_{17MePh}}ZnR][A]$ have also been reported, and although polylactide was obtained under mild reaction conditions (2–4 h, 40 °C), only a slight heterotactic bias was observed ($P_r = 0.51–0.63$).[67]

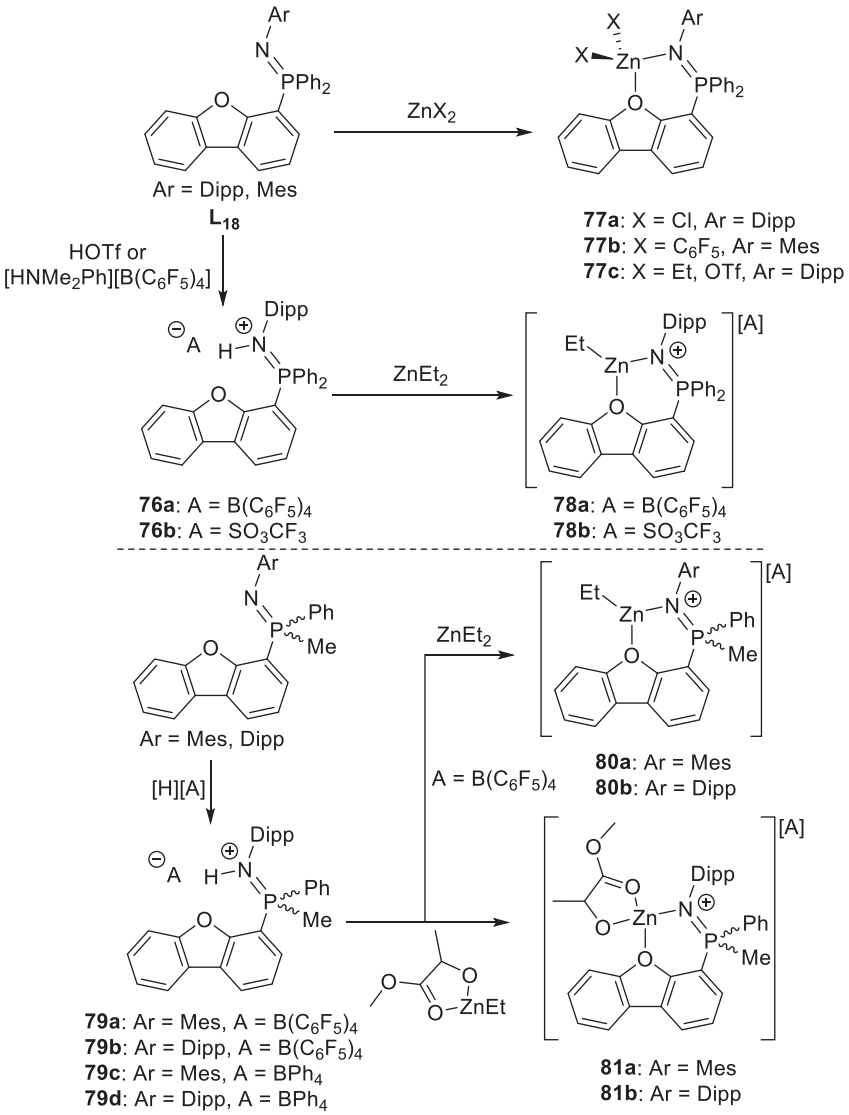

Scheme 26 Synthesis of neutral, cationic and P-stereogenic zinc complexes **77**, **78**, **80** and **81**.[64–66]

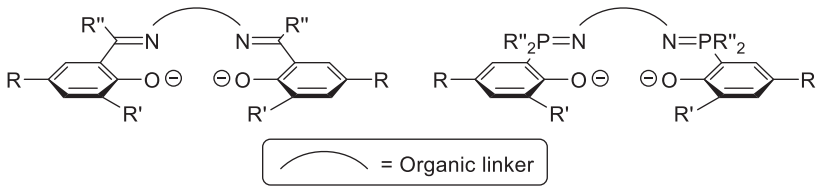

Fig. 4 General structures of salen (left) and phosphasalen (right) ligands. R, R′, R″ and the organic linker vary greatly.

1.07.2.5 Tetradentate Ligands

1.07.2.5.1 Salen-based ligands

Salen ligands are widely used because of their well reported syntheses, combination of hard and soft donors, the chelate effect resulting from typical tetradentate coordination, and oxygen and moisture stability.[68,69] By substituting an imine with a phosphinimine, a new series of scaffolds, dubbed "phosphasalen" ligands (Fig. 4) have been developed by the Williams, Diaconescu and Auffrant research groups, the latter of which recently provided a thorough review on this work in memory of Professor Pascal Le Floch.[70] Most recently, phosphazidosalen and phosphasalen ligand salts were prepared by reaction of the vicinal diazide 1,2-$(N_3)_2$-C_6H_4 with two equivalents of 2–(OK–C_6H_4)PPh_2.[71] Accordingly, this chapter will focus upon the use of alternative tetradentate phosphasalen-like ligands that feature one or more phosphinimine moieties.

1.07.2.5.2 Phosphasalen-like ligands

Scaffolds similar to the previously discussed phosphasalen ligands were created by Le Floch and co-workers, wherein neutral donors, including phosphorus ($[CH_2N{=}PPh_2CH_2PPh_2]_2$, **$L_{19P}$**), sulfur ($[CH_2N{=}PPh_2CH_2PPh_2{=}S]_2$, **$L_{19S}$**) and oxygen ($[CH_2N{=}PPh_2CH_2PPh_2{=}O]_2$, **$L_{19O}$**) have replaced the anionic alkoxides (Scheme 27).[72] An array of iron complexes of these

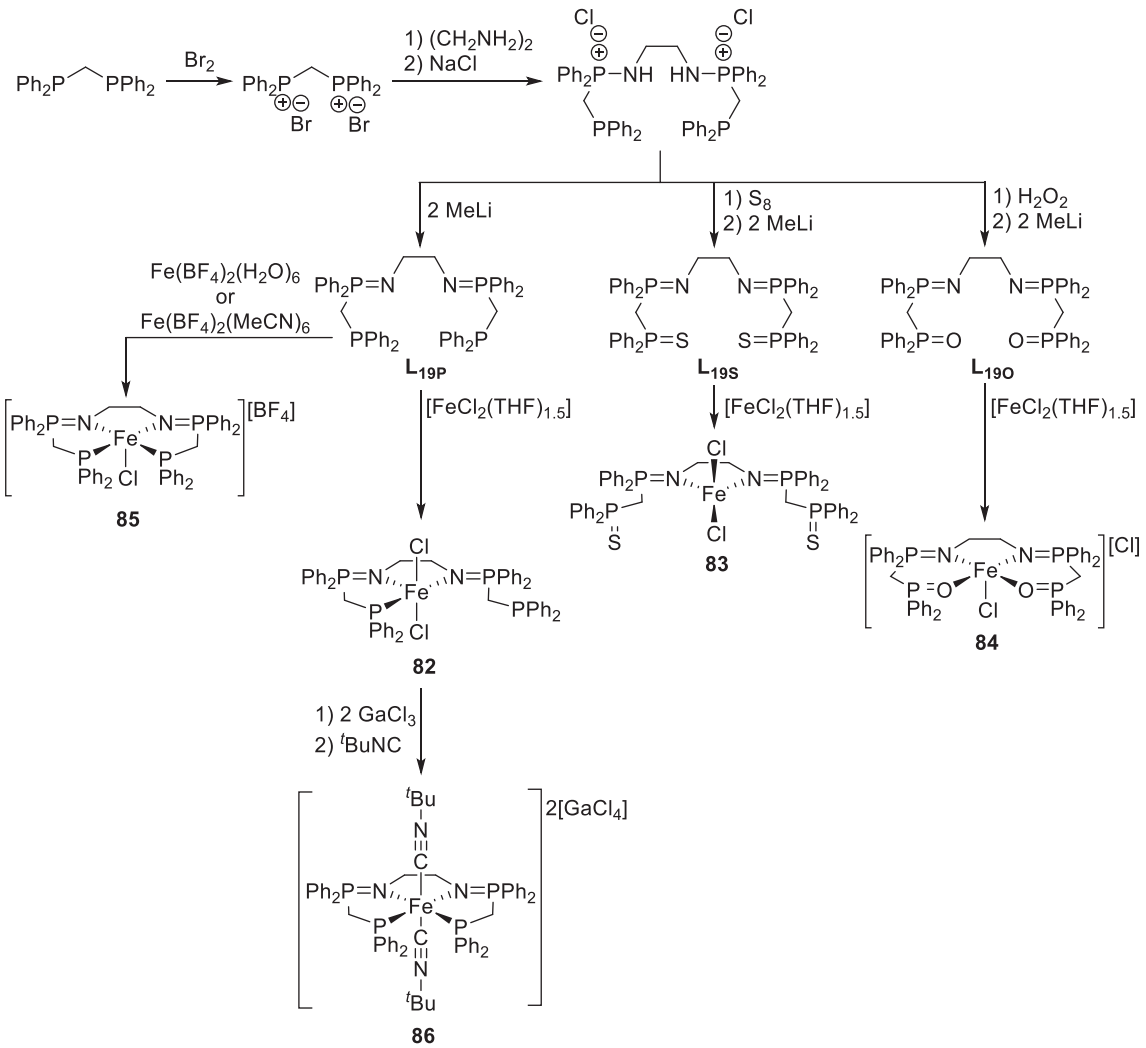

Scheme 27 Synthesis of a phosphasalen-like ligands **L_{19}** and iron complexes (**82–86**) thereof.[72]

ligands were prepared which exhibit a range of bonding modes and geometries, such as trigonal pyramidal (*PNN*-$\mathbf{L_{19P}}FeCl_2$, **82**), tetrahedral (*NN*-$\mathbf{L_{19S}}FeCl_2$, **83**), square based pyramid ($\mathbf{L_{19O}}FeCl$, **84**, $[\mathbf{L_{19P}}FeCl][BF_4]$, **85**) and pseudo octahedral ($[L_{19P}Fe(CN^tBu)_2][GaCl_4]_2$, **86**). These iron complexes demonstrated high activity at low loading (0.1 mol%) for the catalytic hydrogenation of acetophenone; substantially greater turnover numbers were recorded, as compared to previously reported iron catalysts.[73,74]

The diphosphine ligand $\mathbf{L_{19P}}$ was also used to support group 10 elements.[75] Nickel, $[\mathbf{L_{19P}}Ni][Br]_2$, **87**, and palladium, $[\mathbf{L_{19P}}Pd][Cl]_2$, **88**, complexes were synthesized by treating the free ligand with the appropriate metal starting material (Scheme 28). Dicationic square planar complexes were isolated with weakly coordinating bromide (**87**) and chloride (**88**) counterions. Both complexes were found to be stable toward moisture, allowing the pursuit of aqueous reaction chemistry, a rare opportunity for *N,P*-chelates of group 10 metals. Palladium complex **88** was found to be more active mediating Suzuki-Miyaura coupling reactions than **87**, and was established to be a viable catalyst for up to four consecutive reactions.[75]

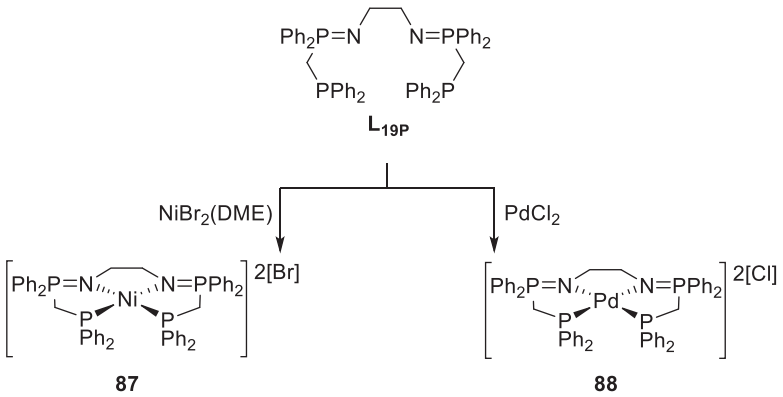

Scheme 28 Synthesis of group 10 complexes **87** and **88**.[75]

The group 9 metal rhodium has also been supported with $\mathbf{L_{19P}}$ (Scheme 29).[76] Utilization of standard rhodium-containing starting materials provided access to $[\mathbf{L_{19P}}Rh][A]$, **89a**: A = Cl; **89b**: A = BF_4. Oxidation of the rhodium center to Rh(III) was achieved by exposure of **89b** to the chloride sources LiCl or C_2Cl_6, affording $[\mathbf{L_{19P}}RhCl_2][BF_4]$, **90**. The related trichloride species $[\mathbf{L_{19P}}RhCl_2][Cl]$, **91**, was obtained by direct reaction of $\mathbf{L_{19P}}$ with $RhCl_3(THT)_3$ (THT = tetrahydrothiophene). A rhodium hydride was postulated to be synthesized by the addition of phenylsilane to complex **91**, given that a doublet with Rh–H coupling ($^1J_{Rh-H}$ = 19.0 Hz) was observed at δ −16.18 in the ^1H NMR spectrum. Unfortunately, neither pure samples nor X-ray quality crystals of $\mathbf{L_{19P}}RhH$, **92**, were obtained.[76]

A variety of $\mathbf{L_{19P}}$-supported ruthenium complexes have also been reported (Scheme 29).[77] Notably, $\mathbf{L_{19P}}RuClH$, **93**, and $[\mathbf{L_{19P}}RuH][B(3,5\text{-}(CF_3)_2C_6H_3)_4]$, **94**, were found to function as pre-catalysts for the transfer hydrogenation of acetophenone. Complex **93** proved to be both more active and robust under various conditions, such as in the presence of sodium isopropoxide or dynamic dihydrogen. Selective abstraction of the chloride and hydride ligands was also achieved to give $[\mathbf{L_{19P}}RuH][O^iPr]$, **95**, and $[\mathbf{L_{19P}}RuCl][A]$, **96a**: [A] = $B(3,5\text{-}(CF_3)_2C_6H_3)_4$, **96b**: [A] = BF_4, respectively.[77]

Several phosphinimine ligands were prepared by Wang et al., and although they focused attention upon the monophosphinimine scaffold 1-—Me-—2-($SiMe_3N{=}PPh_2$)C_6H_4, neutral and anionic bisphosphinimine versions $Me_2Si(CH_2\text{-}2\text{-}(SiMe_3N{=}PPh_2)C_6H_4)_2$, $\mathbf{L_{20}}$, and $Me_2Si(LiCH\text{-}2\text{-}(SiMe_3N{=}PPh_2)C_6H_4)_2$, $Li_2\mathbf{L_{20}}$, which contain an $SiMe_2$ anchor, were also synthesized (Scheme 30).[78] Although $\mathbf{L_{20}}$ has not yet been used for coordination chemistry, the scaffold, especially given the ease and apparent generality of its preparation, holds much promise. In addition, Wang and co-workers have created a substantial body of work using monophosphinimine ligands which the reader is encouraged to investigate.

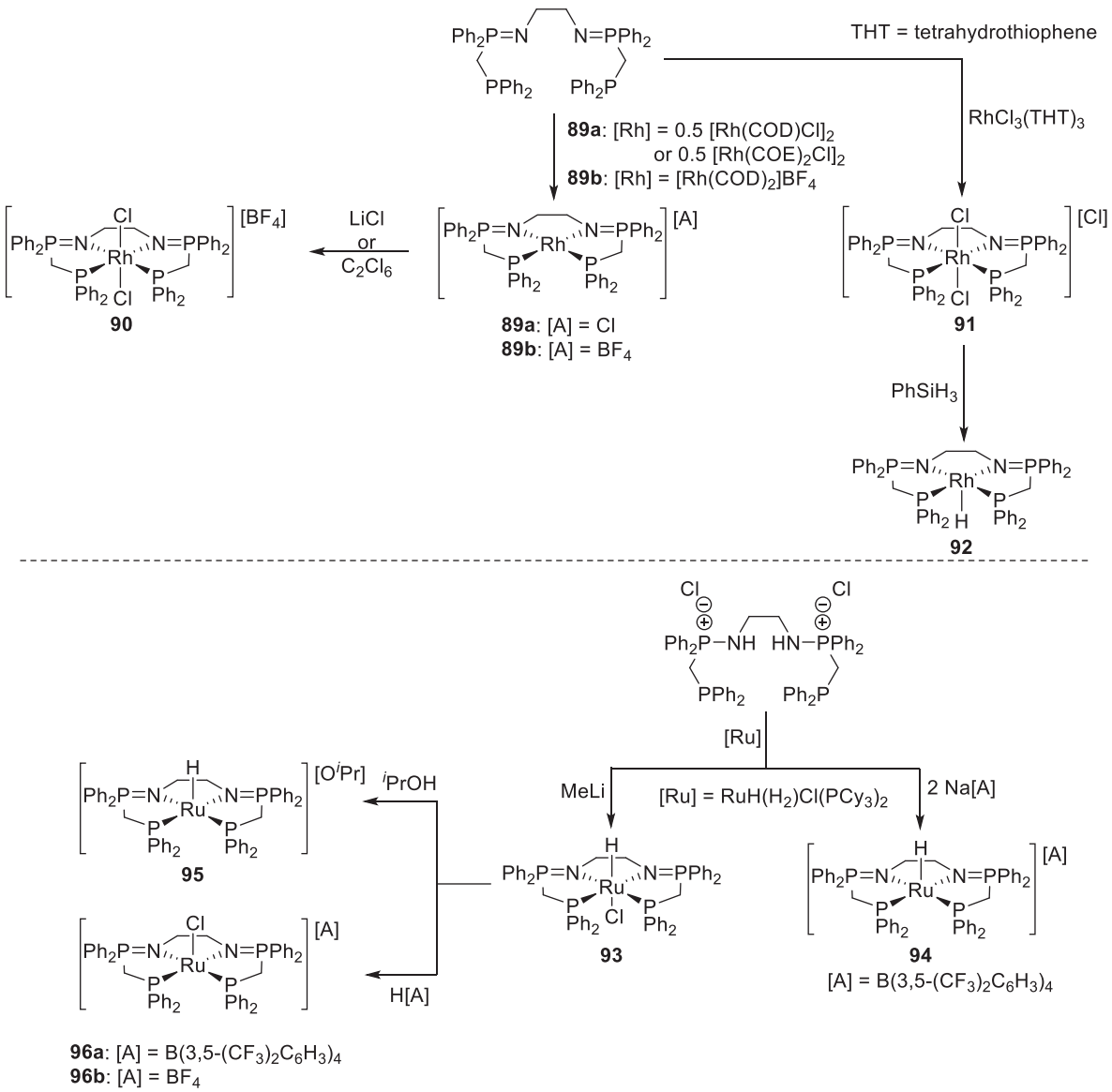

Scheme 29 Synthesis of rhodium (**89–92**) and ruthenium (**93–96**) complexes supported by phosphasalen-like ligand $\mathbf{L_{19P}}$.[76]

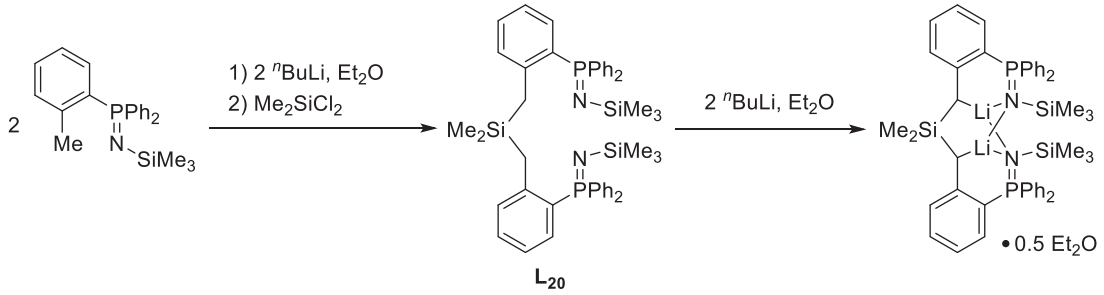

Scheme 30 Synthesis of $Li_2\mathbf{L_{20}}$.[78]

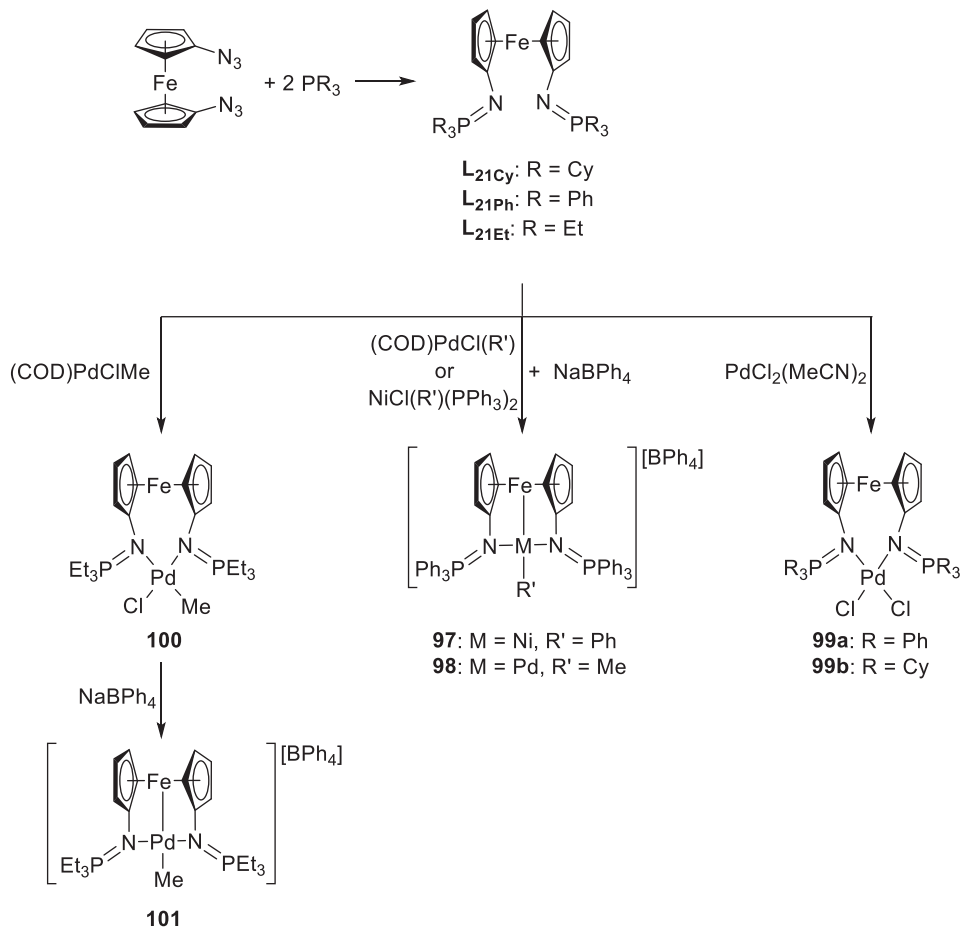

Scheme 31 Group 10 complexes **97–101** which feature bisphosphinimine ferrocene ligands.[79,80]

1.07.2.6 Ferrocene-Containing Ligands

By incorporating a ferrocene moiety into the backbone of a ligand it is possible to create a redox-active ligand. In addition, the η^6 bonding within the iron "sandwich" complex, provides rotational flexibility. The *exo* bisphosphinimine ligand, 1,6-$(N{=}PR_3)_2$ferrocene, $\mathbf{L_{21}}$, which can be prepared by addition of two equivalents of a phosphine to 1,6-$(N_3)_2$ferrocene, has been used as a scaffold for late metals, such as $[\mathbf{L_{21Ph}}NiPh][BPh_4]$, **97**, $[\mathbf{L_{21Ph}}PdMe][BPh_4]$, **98**, $\mathbf{L_{21Ph}}PdCl_2$, **99a**, $\mathbf{L_{21Cy}}PdCl_2$, **99b**, and $\mathbf{L_{21Et}}PdClMe$, **100** (Scheme 31).[79,80] The complex $[\mathbf{L_{21Et}}PdMe][BPh_4]$, **101**, as well as the related ion pairs **97** and **98**, were either redox inactive (**101**, **97**) or underwent an irreversible oxidation (**98**) due to strong dative iron-metal interactions. Attempts to separate the two metal centers with weak nucleophiles, such as acetonitrile and olefins, were unsuccessful.[79,80]

Substituted bisphosphinimine 1,6-$(ArN{=}PPh_2)_2$-2-(CH(Me)R)-ferrocene, $\mathbf{L_{22}}$, and monophosphinimine, 1-(PPh_2)-2-(CH(Me)NMe_2)-6-$(ArN{=}PPh_2)$-ferrocene, $\mathbf{L_{23}}$, and 1-(PR_2)-2-(CH(Me)$N{=}PPh_3$), $\mathbf{L_{24}}$, complexes of group 9 and 10 metals were reported by Kim et al. (Scheme 32).[81] The ferrocene moieties in the *endo* rhodium species $[\mathbf{L_{22}}RhNBD][ClO_4]$, **102a**, and $[\mathbf{L_{22}}RhCOD][BF_4]$, **102b**, and *exo* $[\mathbf{L_{24}}RhNBD][ClO_4]$, **104a**, and $[\mathbf{L_{24}}RhCOD][BF_4]$, **104b**, do not contribute to chemical reactivity, despite introducing chirality to the systems. However, when the chiral monophosphinimine ligands were used in combination with $Rh(NBD)_2BF_4$ for catalyzing hydrogenation reactions, high enantioselectivity (*ee*'s up to 99%) of select olefinic acids (e.g. (*E*)-2-methylcinnamic acid, methyl (*Z*)-2-acetamidocinnamate and methyl (*Z*)-2-acetamidoacrylate) were recorded.

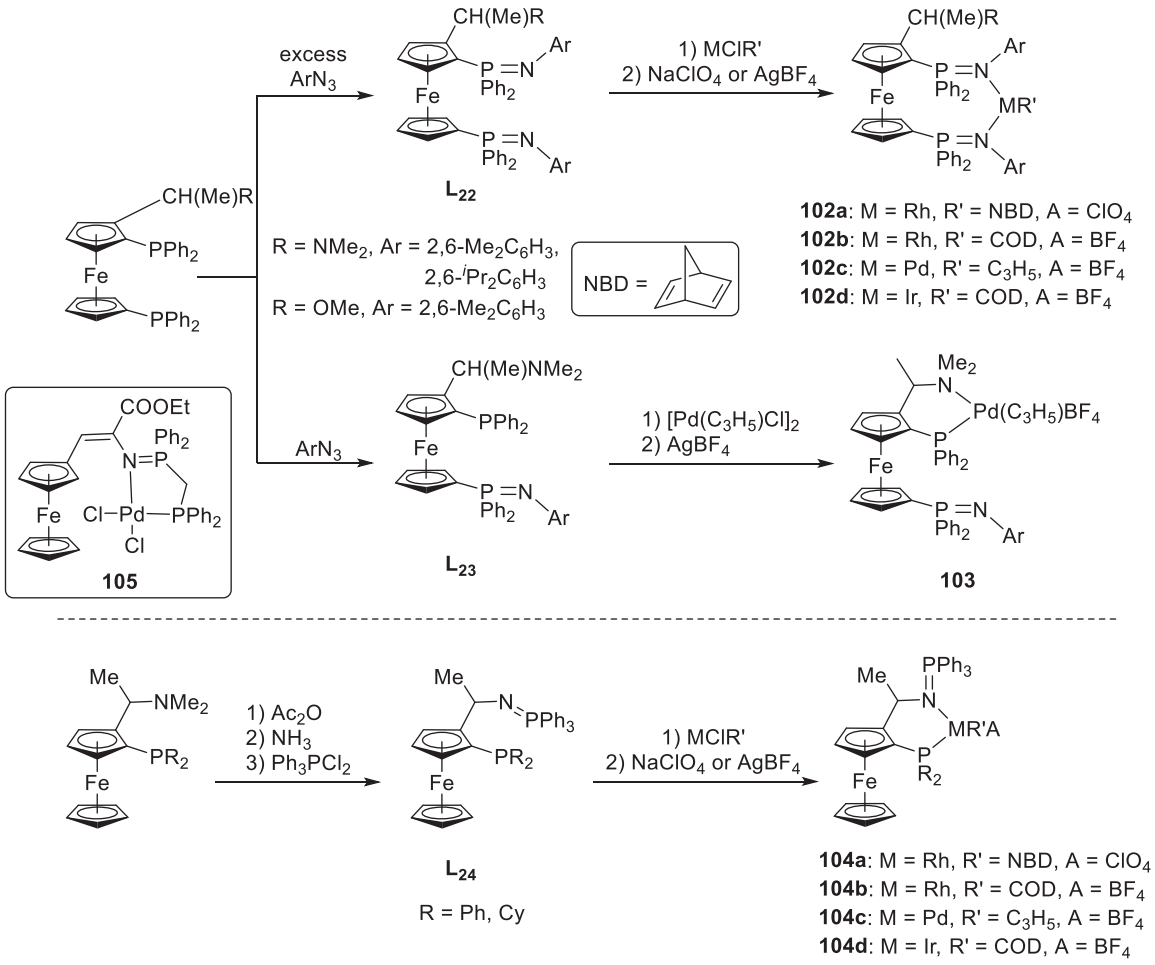

Scheme 32 Use of ferrocene-containing phosphinimine ligands $\mathbf{L_{22}}$-$\mathbf{L_{24}}$ to generate late metal complexes **102–105**.[81–83]

The related palladium complexes [$\mathbf{L_{22}}PdC_3H_5$][BF_4], **102c**, [$\mathbf{L_{23}}PdC_3H_5$][BF_4], **103**, and [$\mathbf{L_{24}}PdC_3H_5$][BF_4], **104c**, were also prepared, and together with several rhodium species, were found to catalyze regioselective allylic alkylation within 24 h; the palladium complexes gave higher yields, but rhodium provided greater *ee's*.[82]

The iridium complexes [$\mathbf{L_{22}}$IrCOD][BF_4], **102d**, and [$\mathbf{L_{24}}$IrCOD][BF_4], **104d**, exhibited catalytic competence for the asymmetric hydrogenation of di- and trisubstituted olefins. Notably, the rhodium species **102b** and **104b** gave rise to more consistent yields for trisubstituted substrates, though *ee*'s were lower.[83]

Ruthenium complexes supported by $\mathbf{L_{22}}$ were prepared in situ as catalysts for asymmetric cyclopropanation of styrene and other olefins. Moderate yields and good enantiomeric excesses were obtained for both *cis* and *trans* olefins.[84] It should be noted that these ruthenium complexes were not isolated and were used at a concentration of 2 mol% with either 1 or 2 equivalents of ligand. A similar study explored in situ generation of copper complexes with $\mathbf{L_{22}}$-$\mathbf{L_{24}}$ for use in asymmetric allylic oxidation of cyclic alkenes and 1,5-cyclooctadiene; the former gave low yields and reasonable *ee*'s, while the latter afforded both good yields and *ee*'s.[85] The related palladium complex [1-CH=C(CO_2Et)N=$PPh_2CH_2PPh_2$-ferrocene]$PdCl_2$, **105**, successfully mediated Sonogashira reactions with highly variable substrates (aromatic and heteroaromatic iodides and bromides with phenyl and ferrocenylacetylene, and aryl bromides and iodides with protected acetylenes).[86]

Several ferrocene-based phosphinimine frameworks (1-(Me_3SiN=P^tBu_2)CpH_4–Fe–Cp(R)$_5$, $\mathbf{L_{25}}$, and 1,6-(Me_3SiN=P^tBu_2)$_2$ferrocene, $\mathbf{L_{26}}$), which upon reaction with titanium chlorides lose Me_3SiCl to serve as anionic phosphinimide ligands, were reported by Stephan in 2010 (Scheme 33).[87] Although these phosphinimides will not be discussed in detail, they are briefly mentioned here to demonstrate the versatility of this class of ligand. Specifically, mono-, $\mathbf{L_{25}}TiCp^{\#}Cl_2$, **106**, and bisphosphinimide, $\mathbf{L_{26}}TiCl_2$, **111**, and $\mathbf{L_{26}}(TiR'Cl_2)_2$, **113**, titanium complexes were synthesized as outlined in Scheme 33.[87] Addition of Grignard reagents to **106**, **111**

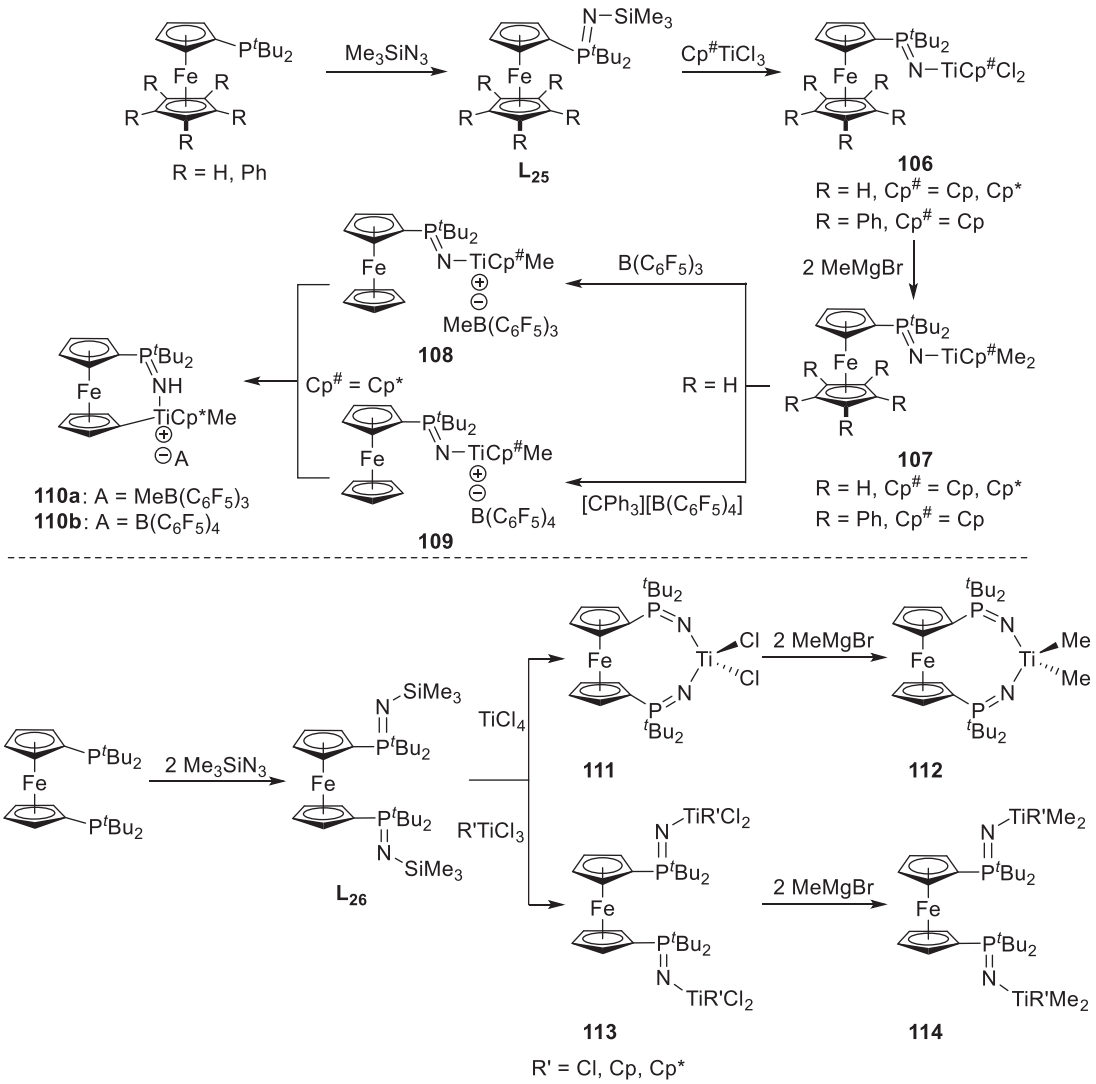

Scheme 33 Synthesis of mono- and bisphosphinimide titanium complexes **106–114**.[87]

and **113** yielded the corresponding organometallic complexes $\mathbf{L_{25}}TiCp^{\#}Me_2$, **107**, $\mathbf{L_{26}}TiMe_2$, **112**, and $\mathbf{L_{26}}(TiR'Me_2)_2$, **114**, respectively. Cationic species $[\mathbf{L_{25}}TiCp^{\#}Me][MeB(C_6F_5)_3]$, **108**, and $[\mathbf{L_{25}}TiCp^{\#}Me][B(C_6F_5)_4]$, **109**, were prepared via methide abstraction from **107**. These ion pairs were prone to Cp C–H activation to afford [*NC*-$\mathbf{L_{25NH}}$TiCp][A], **110a**: A = $MeB(C_6F_5)_3$; **110b**: A = $B(C_6F_5)_4$, as well as several minor unidentified products.[87]

Related sandwich structures featuring two phosphinimine groups have displayed charge-transfer transitions and selective zinc ion sensing properties.[88] The ruthenocene based ligand, 1,6-$(N{=}PPh_3)_2$ruthenocene, $\mathbf{L_{27}}$, was utilized to generate the palladium complex $[\mathbf{L_{27}}PdCl][Cl]$, **115** (Scheme 34). Pseudo-*trans* coordination between the ruthenium and the palladium metal centers was postulated, implying a N–Pd–N bond angle ≅ 180°. X-ray quality crystals were not obtained, and therefore the exact coordination of the metal centers was not confirmed. The ruthenium sandwich ligand $\mathbf{L_{27}}$ was linked to ferrocene via two imine groups, the result of which was established by electrochemical, optical and NMR techniques to be highly selective for zinc coordination. The bisferrocene phosphinimine analogue, ferrocene(1,6-$(N{=}PPh_2)_2$)ferrocene, **116**, was also used for zinc and lithium chemosensing.[89]

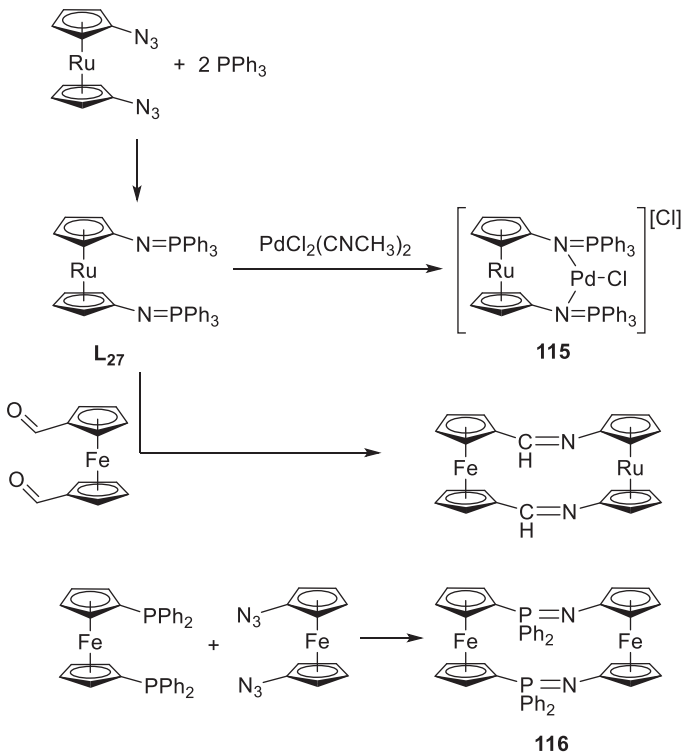

Scheme 34 Synthesis of ruthenocene-based bisphosphinimine ligand $\mathbf{L_{27}}$, and chemistry thereof.[88,89]

1.07.3 Trisphosphinimine Ligands

There are a great number of ligand backbones which incorporate one phosphinimine, and there is also a relatively large variety of systems with two phosphinimines. Examples of more than two, however, are quite rare. Noels et al. used a similar structure to carbon-based analogues of trispyrazolylborate, Tp, ligands to generate the *exo* trisphosphinimine scaffold $R'C(CH_2N{=}PR_3)_3$, $\mathbf{L_{28}}$ (Scheme 35).[28,90,91] The researchers synthesized palladium ($\mathbf{L_{28Ph,Ph}PdCl_2}$, **117a**, and $\mathbf{L_{28Ph,Me}PdCl_2}$, **117b**) and copper ($\mathbf{L_{28}Cu(OTf)_2}$, **118a-d**) complexes of $\mathbf{L_{28}}$ and tested their potential for catalyzing the cyclopropanation of styrene at 60 °C. Similar results were observed to related bisphosphinimine complexes (Scheme 5), wherein the palladium species performed less effectively than their copper congeners over the course of the 3 h experiments. Notably, the ligand substituents did not greatly impact the overall success of the catalyst. The most active catalyst proved to be $\mathbf{L_{28Ph,Me}Cu(OTf)_2}$, **118b**, which also yielded high selectivity (97%) for the desired reaction.[28] The same ligands were later used to synthesize copper (I) ($\mathbf{L_{28}}$CuBr, **119**), iron ($\mathbf{L_{28Ph,Ph}FeCl_2}$, **120**) and nickel ($\mathbf{L_{28}NiBr_2}$, **121**) complexes.[90] A select few, alongside the previously mentioned palladium and copper complexes **117a**, **118a**, **120**, **121a-d**, were tested for their ability to oligomerize ethylene upon addition of the aluminium co-catalysts $[(CH_3)_{0.95}$(n-

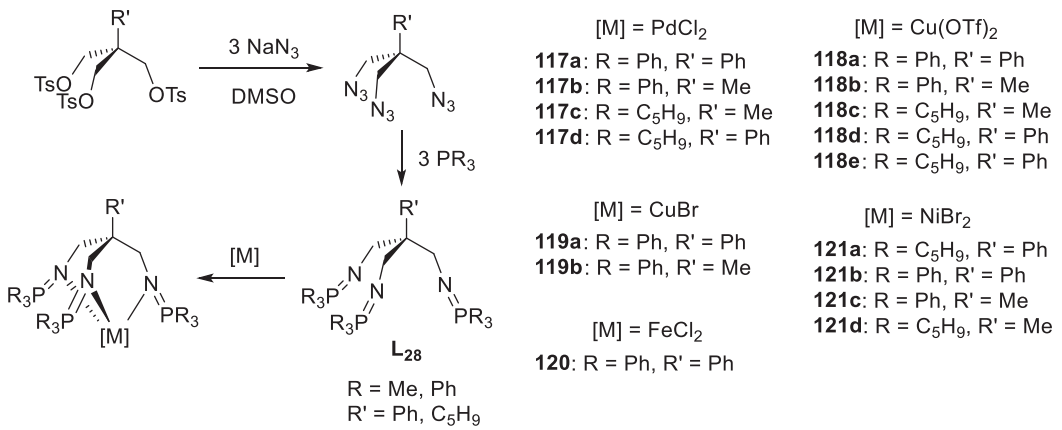

Scheme 35 Synthesis of trisphosphinimine complexes **117–121**.[28,90,91]

$C_8H_{17})_{0.05}AlO]_n$, Et_2AlCl and $EtAlCl_2$.[90,91] The metal, type of aluminium co-catalyst and ligand substituents did not affect ethylene consumption, but did govern oligomer distribution, with the palladium catalyst **117a** giving standout discrimination (93%) for hexenes.

1.07.4 Conclusions

In this chapter, the synthesis and coordination chemistry of bis- and trisphosphinimine-containing ligands reported over the past 15 years (2004–19) has been surveyed. Two predominant synthetic strategies have been employed to yield the plethora of frameworks that bear multiple phosphinimine functionalities; the variety of ligand backbones, phosphorus and nitrogen substituents, and additional donor groups continues to expand rapidly. These phosphinimine-containing ligands have been used to support the vast majority of metals across the periodic table, unlocking a wealth of coordination chemistry that will surely continue to prosper.

References

1. Hanson, S. S.; Doni, E.; Traboulsee, K. T.; Coulthard, G.; Murphy, J. A.; Dyker, C. A. *Angew. Chem. Int. Ed.* **2015,** *54* (38), 11236–11239.
2. Abel, E. W.; Mucklejohn, S. A. *Phosphorus Sulfur Silicon Relat. Elem.* **1981,** *9* (3), 235–266.
3. Cariou, R.; Graham, T. W.; Dahcheh, F.; Stephan, D. W. *Dalton Trans.* **2011,** *40* (20), 5419–5422.
4. Staudinger, H.; Meyer, J. *Helv. Chim. Acta* **1919,** *2* (1), 635–646.
5. Gololobov, Y. G.; Zhmurova, I. N.; Kasukhin, L. F. *Tetrahedron* **1981,** *37* (3), 437–472.
6. Gololobov, Y. G.; Kasukhin, L. F. *Tetrahedron* **1992,** *48* (8), 1353–1406.
7. Bebbington, M. W. P.; Bourissou, D. *Coord. Chem. Rev.* **2009,** *253* (9), 1248–1261.
8. Eguchi, S.; Matsushita, Y.; Yamashita, K. *Org. Prep. Proced. Int.* **1992,** *24* (2), 209–243.
9. Meng, G.; Guo, T.; Ma, T.; Zhang, J.; Shen, Y.; Sharpless, K. B.; Dong, J. *Nature* **2019,** *574* (7776), 86–89.
10. Ong, C. M.; McKarns, P.; Stephan, D. W. *Organometallics* **1999,** *18* (20), 4197–4204.
11. Steiner, A.; Zacchini, S.; Richards, P. I. *Coord. Chem. Rev.* **2002,** *227* (2), 193–216.
12. Vicente, J.; Abad, J.-A.; Clemente, R.; López-Serrano, J.; Ramírez de Arellano, M. C.; Jones, P. G.; Bautista, D. *Organometallics* **2003,** *22* (21), 4248–4259.
13. Cavell, R. G.; Kamalesh Babu, R. P.; Aparna, K. *J. Organomet. Chem.* **2001,** *617-618,* 158–169.
14. Jones, N. D.; Cavell, R. G. *J. Organomet. Chem.* **2005,** *690* (24), 5485–5496.
15. Roesky, P. W. *Z. Anorg. Allg. Chem.* **2006,** *632* (12 – 13), 1918–1926.
16. Panda, T. K.; Roesky, P. W. *Chem. Soc. Rev.* **2009,** *38* (9), 2782–2804.
17. Liddle, S. T.; Mills, D. P.; Wooles, A. J. *Organometallic Chemistry*; ; The Royal Society of Chemistry, 2010; pp 29–55.
18. Hadrien, H.; Marie, F.; Audrey, A.; Nicolas, M. *Lett. Org. Chem.* **2010,** *7* (8), 596–611.
19. Harder, S. *Coord. Chem. Rev.* **2011,** *255* (11), 1252–1267.
20. Liddle, S. T.; Mills, D. P.; Wooles, A. J. *Chem. Soc. Rev.* **2011,** *40* (5), 2164–2176.
21. Gregson, M.; Wooles, A. J.; Cooper, O. J.; Liddle, S. T. *Comments Inorg. Chem.* **2015,** *35* (5), 262–294.
22. Chavagnan, T.; Bauder, C.; Sémeril, D.; Matt, D.; Toupet, L. *Eur. J. Org. Chem.* **2017,** *2017* (1), 70–76.
23. Monnereau, L.; Sémeril, D.; Matt, D. *Adv. Synth. Catal.* **2013,** *355* (7), 1351–1360.
24. Monnereau, L.; Sémeril, D.; Matt, D. *Eur. J. Org. Chem.* **2012,** *2012* (14), 2786–2791.
25. Xiong, Y.; Yao, S.; Inoue, S.; Berkefeld, A.; Driess, M. *Chem. Commun.* **2012,** *48* (100), 12198–12200.
26. Xiong, Y.; Yao, S.; Inoue, S.; Irran, E.; Driess, M. *Angew. Chem. Int. Ed.* **2012,** *51* (40), 10074–10077.
27. Kögel, J. F.; Xie, X.; Baal, E.; Gesevičius, D.; Oelkers, B.; Kovačević, B.; Sundermeyer, J. *Chem. A Eur. J.* **2014,** *20* (25), 7670–7685.
28. Beaufort, L.; Demonceau, A.; Noels, A. F. *Tetrahedron* **2005,** *61* (38), 9025–9030.
29. Sgro, M. J.; Stephan, D. W. *Dalton Trans.* **2011,** *40* (11), 2419–2421.
30. Oulié, P.; Nebra, N.; Saffon, N.; Maron, L.; Martin-Vaca, B.; Bourissou, D. *J. Am. Chem. Soc.* **2009,** *131* (10), 3493–3498.
31. Cariou, R.; Dahcheh, F.; Graham, T. W.; Stephan, D. W. *Dalton Trans.* **2011,** *40* (18), 4918–4925.
32. Cariou, R.; Graham, T. W.; Stephan, D. W. *Dalton Trans.* **2013,** *42* (12), 4237–4239.
33. Chai, Z.-Y.; Zhang, C.; Wang, Z.-X. *Organometallics* **2008,** *27* (7), 1626–1633.
34. Wang, Z.-X.; Wang, L. *Chem. Commun.* **2007**, (23), 2423–2425.
35. Wang, L.; Wang, Z.-X. *Org. Lett.* **2007,** *9* (21), 4335–4338.
36. Alt, H. G.; Schneider, K. J.; Funk, E. *Jordan J. Chem.* **2008,** *3* (4), 367–379.
37. Cheisson, T.; Auffrant, A. *Dalton Trans.* **2014,** *43* (35), 13399–13409.
38. Hänninen, M. M.; Zamora, M. T.; MacNeil, C. S.; Knott, J. P.; Hayes, P. G. *Chem. Commun.* **2016,** *52* (3), 586–589.
39. MacNeil, C. S.; Glynn, K. E.; Hayes, P. G. *Organometallics* **2018,** *37* (19), 3248–3252.
40. MacNeil, C. S.; Hayes, P. G. *Chem. Eur. J.* **2019,** *25* (35), 8203–8207.
41. Rong, W.; Cheng, J.; Mou, Z.; Xie, H.; Cui, D. *Organometallics* **2013,** *32* (19), 5523–5529.
42. Rong, W.; Wang, M.; Li, S.; Cheng, J.; Liu, D.; Cui, D. *Organometallics* **2018,** *37* (6), 971–978.
43. Rong, W.; Liu, D.; Zuo, H.; Pan, Y.; Jian, Z.; Li, S.; Cui, D. *Organometallics* **2013,** *32* (5), 1166–1175.
44. Rong, W.; He, D.; Wang, M.; Mou, Z.; Cheng, J.; Yao, C.; Li, S.; Trifonov, A. A.; Lyubov, D. M.; Cui, D. *Chem. Commun.* **2015,** *51* (24), 5063–5065.
45. Johnson, K. R. D.; Hayes, P. G. *Organometallics* **2009,** *28* (21), 6352–6361.
46. Johnson, K. R. D.; Hayes, P. G. *Organometallics* **2013,** *32* (15), 4046–4049.
47. Johnson, K. R. D.; Hayes, P. G. *Dalton Trans.* **2014,** *43* (6), 2448–2457.
48. Johnson, K. R. D.; Hayes, P. G. *Inorg. Chim. Acta* **2014,** *422,* 209–217.
49. Johnson, K. R. D.; Kamenz, B. L.; Hayes, P. G. *Can. J. Chem.* **2016,** *94* (4), 330–341.
50. Johnson, K. R. D.; Hayes, P. G. *Organometallics* **2011,** *30* (1), 58–67.
51. Johnson, K. R. D.; Hannon, M. A.; Ritch, J. S.; Hayes, P. G. *Dalton Trans.* **2012,** *41* (26), 7873–7875.
52. Zamora, M. T.; Johnson, K. R. D.; Hänninen, M. M.; Hayes, P. G. *Dalton Trans.* **2014,** *43* (28), 10739–10750.

53. Knott, J. P.; Hänninen, M. M.; Rautiainen, J. M.; Tuononen, H. M.; Hayes, P. G. *J. Organomet. Chem.* **2017,** *845,* 135–143.
54. Cheisson, T.; Auffrant, A.; Nocton, G. *Organometallics* **2015,** *34* (22), 5470–5478.
55. Cheisson, T.; Ricard, L.; Heinemann, F. W.; Meyer, K.; Auffrant, A.; Nocton, G. *Inorg. Chem.* **2018,** *57* (15), 9230–9240.
56. Chai, Z.-Y.; Wang, Z.-X. *Dalton Trans.* **2009**, (38), 8005–8012.
57. Wheaton, C. A.; Hayes, P. G. *Dalton Trans.* **2010,** *39* (16), 3861–3869.
58. Wheaton, C. A.; Hayes, P. G. *Chem. Commun.* **2010,** *46* (44), 8404–8406.
59. Wheaton, C. A.; Hayes, P. G. *Cat. Sci. Technol.* **2012,** *2* (1), 125–138.
60. Wheaton, C. A.; Hayes, P. G. *J. Organomet. Chem.* **2012,** *704,* 65–69.
61. Zamora, M. T.; Zahir, S. M.; Johnson, K. R. D.; Barnson, C. J.; Wheaton, C. A.; Hänninen, M. M.; Hayes, P. G. *Aust. J. Chem.* **2015,** *68* (3), 373–384.
62. Ireland, B. J.; Wheaton, C. A.; Hayes, P. G. *Organometallics* **2010,** *29* (5), 1079–1084.
63. Wheaton, C. A.; Hayes, P. G. *Comments Inorg. Chem.* **2011,** *32* (3), 127–162.
64. Wheaton, C. A.; Ireland, B. J.; Hayes, P. G. *Z. Anorg. Allg. Chem.* **2011,** *637* (14–15), 2111–2119.
65. Wheaton, C. A.; Ireland, B. J.; Hayes, P. G. *Organometallics* **2009,** *28* (5), 1282–1285.
66. Sun, H.; Ritch, J. S.; Hayes, P. G. *Inorg. Chem.* **2011,** *50* (17), 8063–8072.
67. Sun, H.; Ritch, J. S.; Hayes, P. G. *Dalton Trans.* **2012,** *41* (13), 3701–3713.
68. Pfeiffer, P.; Breith, E.; Lübbe, E.; Tsumaki, T. *Justus Liebigs Ann. Chem.* **1933,** *503* (1), 84–130.
69. Tokuichi, T. *Bull. Chem. Soc. Jpn.* **1938,** *13* (2), 252–260.
70. Marín, I. M.; Auffrant, A. *Eur. J. Inorg. Chem.* **2018,** *2018* (15), 1634–1644.
71. Dickie, T. K. K.; MacNeil, C. S.; Hayes, P. G. *Dalton Trans.* **2020**, (49), 578–582.
72. Buchard, A.; Heuclin, H.; Auffrant, A.; Le Goff, X. F.; Le Floch, P. *Dalton Trans.* **2009**, (9), 1659–1667.
73. Sui-Seng, C.; Freutel, F.; Lough, A. J.; Morris, R. H. *Angew. Chem. Int. Ed.* **2008,** *47* (5), 940–943.
74. Mikhailine, A.; Lough, A. J.; Morris, R. H. *J. Am. Chem. Soc.* **2009,** *131* (4), 1394–1395.
75. Buchard, A.; Komly, B.; Auffrant, A.; Le Goff, X. F.; Floch, P. L. *Organometallics* **2008,** *27* (17), 4380–4385.
76. Buchard, A.; Payet, E.; Auffrant, A.; Le Goff, X.; Le Floch, P. *New J. Chem.* **2010,** *34* (12), 2943–2949.
77. Dyer, H.; Picot, A.; Vendier, L.; Auffrant, A.; Le Floch, P.; Sabo-Etienne, S. *Organometallics* **2011,** *30* (6), 1478–1486.
78. Wang, Z.-X.; Qi, C.-Y. *Dalton Trans.* **2005**, (5), 996–1001.
79. Metallinos, C.; Tremblay, D.; Barrett, F. B.; Taylor, N. J. *J. Organomet. Chem.* **2006,** *691* (9), 2044–2047.
80. Abubekerov, M.; Khan, S. I.; Diaconescu, P. L. *Organometallics* **2017,** *36* (22), 4394–4402.
81. Co, T. T.; Shim, S. C.; Cho, C. S.; Kim, T.-J.; Kang, S. O.; Han, W.-S.; Ko, J.; Kim, C.-K. *Organometallics* **2005,** *24* (20), 4824–4831.
82. Co, T. T.; Shim, S.-C.; Cho, C.-S.; Kim, D.-U.; Kim, T.-J. *Bull. Korean Chem. Soc.* **2005,** *26* (9), 1359–1365.
83. Co, T. T.; Kim, T.-J. *Chem. Commun.* **2006**, (33), 3537–3539.
84. Hoang, V. D. M.; Reddy, P. A. N.; Kim, T.-J. *Tetrahedron Lett.* **2007,** *48* (45), 8014–8017.
85. Hoang, V. D. M.; Reddy, P. A. N.; Kim, T.-J. *Organometallics* **2008,** *27* (6), 1026–1027.
86. Arques, A.; Auñon, D.; Molina, P. *Tetrahedron Lett.* **2004,** *45* (22), 4337–4340.
87. Ramos, A.; Stephan, D. W. *Dalton Trans.* **2010,** *39* (5), 1328–1338.
88. Otón, F.; Espinosa, A.; Tárraga, A.; Molina, P. *Organometallics* **2007,** *26* (25), 6234–6242.
89. Otón, F.; Ratera, I.; Espinosa, A.; Wurtz, K.; Parella, T.; Tárraga, A.; Veciana, J.; Molina, P. *Chem. A Eur. J.* **2010,** *16* (5), 1532–1542.
90. Beaufort, L.; Delaude, L.; Noels, A. F. *Tetrahedron* **2007,** *63* (30), 7003–7008.
91. Beaufort, L.; Benvenuti, F.; Delaude, L.; Noels, A. F. *J. Mol. Catal. A Chem.* **2008,** *283* (1), 77–82.